

$B - L$ model with $A_4 \times Z_3 \times Z_4$ symmetry for 3 + 1 active–sterile neutrino mixing

V. V. Vien^{a,b*}

^{a)}*Institute of Applied Technology, Thu Dau Mot University, Binh Duong Province, Vietnam, and*

^{b)}*Department of Physics, Tay Nguyen University, Daklak province, Vietnam.*

(Dated: June 7, 2022)

We construct a $B - L$ model with $A_4 \times Z_3 \times Z_4$ flavor symmetry which can accounts for the recent 3 + 1 active-sterile neutrino data. The tiny neutrino mass and the mass hierarchy are obtained by the type-I seesaw mechanism. The hierarchy of the lepton masses is satisfied by a factor of $v_H \left(\frac{v_L}{\Lambda}\right)^2 \sim 10^{-4}$ GeV of the electron mass compared to the muon and tau masses of the order of $\frac{v_H v_L}{\Lambda} \sim 10^{-1}$ GeV. The 3 + 1 active-sterile neutrino mixings are predicted to be $0.015 \leq |U_{14}|^2 \leq 0.045$, $0.004 \leq |U_{24}|^2 \leq 0.012$ and $0.004 \leq |U_{34}|^2 \leq 0.014$ for normal hierarchy while $0.020 \leq |U_{14}|^2 \leq 0.045$, $0.008 \leq |U_{24}|^2 \leq 0.018$ and $0.008 \leq |U_{34}|^2 \leq 0.022$ for inverted hierarchy. Sterile neutrino masses are predicted to be $0.7 \lesssim m_s$ (eV) $\lesssim 3.16$ for normal hierarchy and $2.6 \lesssim m_s$ (eV) $\lesssim 7.1$ for inverted hierarchy. For three neutrino scheme the model predicts $0.3401 \leq \sin^2 \theta_{12} \leq 0.3415$, $0.460 \leq \sin^2 \theta_{23} \leq 0.540$, $-0.60 \leq \sin \delta_{CP} \leq -0.20$ for normal hierarchy and $0.3402 \leq \sin^2 \theta_{12} \leq 0.3416$, $0.434 \leq \sin^2 \theta_{23} \leq 0.610$, $-0.95 \leq \sin \delta_{CP} \leq -0.60$ for inverted hierarchy.

PACS numbers: 12.15 Ff; 12.60.Fr; 14.60.St.

I. INTRODUCTION

Apart from the current unconfirmed parameters, including the mass hierarchy, the octant of θ_{23} and the Dirac CP phase [1], there exist some experimental results in the neutrino sector that cannot be explained within the three neutrino scheme [2–15]. However, these parameters could be interpreted by adding at least an additional neutrino with mass in the eV range ($\Delta m_{41}^2 \gg |\Delta m_{31}^2|$). The mentioned neutrinos are $SU(2)_L$ singlets that do not contribute to the weak interactions but mix with the active neutrinos which can be probed by experiments.

There have been some schemes with sterile neutrinos proposed in the literature such as (3+1) scheme [16–32], (3+1+1) scheme [33–37], and (1+3+1) scheme [38, 39], (3+2) scheme [40–47], neutrino non-standard interactions [48–52] and radiative sterile neutrino decays [53, 54]. Among four neutrino schemes, the one with three active neutrinos and one sterile neutrino (called 3+1

* vovanvien@tdmu.edu.vn

scheme) is preferred because the 1+3 scenario is disfavored by cosmology and the 2+2 scheme is not compatible with the solar and the atmospheric data [3, 55].

At present, the neutrino parameters in the three neutrino framework [1] and (3+1) neutrino framework [9, 55], for the best-fit values and 3σ range, are given in Table I.

Table I. Neutrino parameters in the three neutrino framework taken from Ref. [1] and (3+1) neutrino framework taken from [9, 55]

Parameters	3σ range (best fit)	
	Normal hierarchy	Inverted hierarchy
$\Delta m_{21}^2(10^{-5} \text{ eV}^2)$	$6.94 \rightarrow 8.14 (7.50)$	$6.94 \rightarrow 8.14 (7.50)$
$ \Delta m_{31}^2 (10^{-3} \text{ eV}^2)$	$2.47 \rightarrow 2.63 (2.55)$	$2.37 \rightarrow 2.53 (2.45)$
$\sin^2 \theta_{12}/10^{-1}$	$2.71 \rightarrow 3.69 (3.18)$	$2.71 \rightarrow 3.69 (3.18)$
$\sin^2 \theta_{23}/10^{-1}$	$4.34 \rightarrow 6.10 (5.74)$	$4.33 \rightarrow 6.08 (5.78)$
$\sin^2 \theta_{13}/10^{-2}$	$2.000 \rightarrow 2.405 (2.200)$	$2.018 \rightarrow 2.424 (2.225)$
δ/π	$0.71 \rightarrow 1.99 (1.08)$	$1.11 \rightarrow 1.96 (1.58)$
$ U_{14} ^2$	$0.012 \rightarrow 0.047$	$0.012 \rightarrow 0.047$
$ U_{24} ^2$	$0.005 \rightarrow 0.03$	$0.005 \rightarrow 0.03$
$ U_{34} ^2$	$0 \rightarrow 0.16$	$0 \rightarrow 0.16$

One outstanding feature of discrete symmetries is imposed to explain the neutrino oscillation data which have been widely used in the literature. Among several discrete symmetries, the A_4 has attracted a lot of attention because it is the smallest symmetry which possesses one three-dimensional representation and three inequivalent one-dimensional representations. Recently, there have been different suggestions for generating the active-sterile neutrino mixing within different works [55–83]. In 3 + 1 framework, the $B - L$ model based on S_3 symmetry was first proposed in Ref. [66] without considering the active-sterile neutrino mixing. This problem has been improved in Ref. [83] in which the active-sterile neutrino mass and mixing are obtained at the first-order of the perturbation theory and only the normal ordering of the active neutrino masses is considered. However, the charged-lepton mass hierarchy is not yet solved in Ref. [83]¹. In Refs. [55–61], based on A_4 symmetry, the active-sterile neutrino mass and mixing have been considered with non minimal scalar sector and many $SU(2)_L$ Higgs doublets, thus there are substantial differences between previous works and our present work. For instance, in Refs. [56, 57] the symmetry of the SM is supplemented by the $A_4 \times Z_3 \times U(1)_R$ symmetry in which two doublets are introduced to get

¹ As will be shown in section IV, the charged-lepton mass hierarchy is naturally explained in the current model.

sterile neutrino mass with the help of the dimension-six terms [56] or the perturbation theory[57]. In order to generate the sterile-active neutrino masses and mixings, in Ref. [58] the symmetry of the SM is supplemented by the $A_4 \times Z_4$ symmetry in which one doublet and up to twelve singlets are introduced but only $|U_{e4}|$ is predicted without $|U_{\mu 4}|$ and $|U_{\tau 4}|$; in Ref. [59], the symmetry of the SM is supplemented by the $A_4 \times Z_3 \times Z'_3 \times U(1)_R$ symmetry in which two doublets and up to seventeen singlets are introduced; in Ref. [60], the symmetry of the SM is supplemented by the $A_4 \times Z_3 \times Z_4$ symmetry² in which three doublets and up to twelve singlets are introduced; in Ref. [61] the symmetry of the SM is supplemented by the $A_4 \times Z_4$ symmetry in which one doublets and up to twelve singlets are introduced, and in Ref. [55] the symmetry of the SM is supplemented by the $A_4 \times C_4 \times C_6 \times C_2 \times U(1)_s$ symmetry in which one doublets and up to twelve singlets are introduced whereby only the normal ordering of the light neutrino masses is predicted. Therefore, it would be necessary to construct an A_4 flavor model with less scalar content than our previous model which satisfies the minimization condition of the scalar potential. To the best of our knowledge, A_4 symmetry has not yet been combined with the $B - L$ model in the 3+1 scheme.

The remainder of this work is structured as follows. The description of the model is presented in section II. The scalar potential of the model is described in section III. The active–sterile neutrino mixing is presented in section IV and section V is devoted to the numerical analysis. Finally, some conclusions are drawn in section VI.

II. THE MODEL

The $B - L$ gauge model³ is extended by the discrete symmetry $A_4 \times Z_3 \times Z_4$. Besides, three right-handed neutrinos (ν_R), one sterile neutrino (ν_s) and three $SU(2)_L$ singlet scalars (ϕ_l, ϕ_ν, ϕ_s) are introduced in addition to the $B - L$ model. In present work, each three left-handed leptons and three right-handed neutrinos are put in one A_4 triplet while each the right-handed charged leptons l_{1R}, l_{2R} and l_{3R} are, respectively, put in $\underline{1}, \underline{1}''$ and $\underline{1}'$ under A_4 , and the sterile neutrino ν_s is put in $\underline{1}$ under A_4 symmetry. The particle content of the considered model, under $\Gamma \equiv SU(3)_C \times SU(2)_L \times U(1)_Y \times U(1)_{B-L} \times A_4 \times Z_3 \times Z_4$ symmetry, is shown in Table II⁴.

From the field assignments given in Tab. II, the following Yukawa terms, up to five-dimension

² In our present work, although the discrete symmetry structure is similar to that of Ref. [60], however, the alignment of fields and the number of scalars are completely different from each other.

³ In the gauge $B - L$ model, the anomalies can be cancelled in various scenarios[91–106] with different charge assignments of $B - L$. In this study, we use the model proposed in Refs. [93, 94]

⁴ All leptons and scalar fields are aligned in singlet **1** of $SU(3)_L$ symmetry.

Table II. The particle and scalar contents of the model.

Fields	ψ_L	l_{1R}	l_{2R}	l_{3R}	H	ϕ_l	ϕ_ν	$\eta(\eta_s)$	ϕ_s	ν_R	ν_s
SU(2) _L	2	1	1	1	2	1	1	1	1	1	1
U(1) _{B-L}	-1	-1	-1	-1	0	0	0	2	0	-1	-1
A_4	3	1	1''	1'	1	3	3	1	3	3	1
Z_3	ω	ω	ω	ω	1	1	1	ω	ω	ω	1
Z_4	i	$-i$	1	-1	1	i	1	-1	-1	i	$-i$

which invariant under Γ symmetry, arise⁵:

$$\begin{aligned} -\mathcal{L}_Y^l = & \frac{x_{1cl}}{\Lambda^2} (\bar{\psi}_L l_{1R})_{\underline{3}} (H \phi_l^2)_{\underline{3}} + \frac{x_{2cl}}{\Lambda} (\bar{\psi}_L l_{2R})_{\underline{3}} (H \phi_l)_{\underline{3}} + \frac{x_{3cl}}{\Lambda} (\bar{\psi}_L l_{3R})_{\underline{3}} (H \phi_l^*)_{\underline{3}} \\ & + x_{1\nu} (\bar{\psi}_L \nu_R)_{\underline{1}} \tilde{H} + \frac{x_{2\nu}}{\Lambda} (\bar{\psi}_L \nu_R)_{\underline{3}_s} (\tilde{H} \phi_\nu)_{\underline{3}} + \frac{x_{3\nu}}{\Lambda} (\bar{\psi}_L \nu_R)_{\underline{3}_a} (\tilde{H} \phi_\nu)_{\underline{3}} \\ & + \frac{y_\nu}{2} (\bar{\nu}_R^c \nu_R)_{\underline{1}} \eta + \frac{y_s}{\Lambda} (\bar{\nu}_s^c \nu_R)_{\underline{3}} (\eta_s \phi_s)_{\underline{3}} + \text{H.c}, \end{aligned} \quad (1)$$

where $x_{1,2,3cl}$, $x_{1,2,3\nu}$, y_ν and y_s are the Yukawa-like dimensionless coupling constants, and Λ is the cut-off scale. The non-Abelian discrete symmetry A_4 along with Abelian symmetries Z_3 and Z_4 play an important role to generate a desired neutrino mass matrix structure consistent with the sterile-active neutrino mixing data. For instance, the charged lepton masses arise from $\bar{\psi}_L l_{1,2,3R}$ to scalars, where under Γ symmetry, $\bar{\psi}_L l_{1R} \sim (\mathbf{2}, -\frac{1}{2}, 0, \underline{3}, 1, -1)$, $\bar{\psi}_L l_{2R} \sim (\mathbf{2}, -\frac{1}{2}, 0, \underline{3}, \omega, -i)$ and $\bar{\psi}_L l_{1R} \sim (\mathbf{2}, -\frac{1}{2}, 0, \underline{3}, 1, i)$. For the known scalars, $\bar{\psi}_L l_{1R} H$ is prevented by three symmetries A_4 , Z_3 and Z_4 ; $\bar{\psi}_L l_{1R} H \phi_l$ is prevented by two symmetries Z_3 and Z_4 ; $\bar{\psi}_L l_{1R} H \phi_l^*$ is prevented by Z_4 symmetry and so on. $\bar{\psi}_L l_{2R} H$ is prevented by A_4 , Z_3 and Z_4 symmetries; $\bar{\psi}_L l_{2R} H \phi_\nu$ is prevented by Z_3 and Z_4 symmetries and so on. $\bar{\psi}_L l_{3R} H$ is prevented by A_4 , Z_3 and Z_4 symmetries; $\bar{\psi}_L l_{3R} H \phi_l$ is prevented by Z_3 and Z_4 symmetries; $\bar{\psi}_L l_{3R} H \eta$ is prevented by A_4 , Z_3 and Z_4 symmetries; $\bar{\psi}_L l_{3R} \phi_s$ is prevented by Z_3 and Z_4 symmetries and so on. Thus, under Γ symmetry, there is only three invariant terms $(\bar{\psi}_L l_{1R})_{\underline{3}} (H \phi_l^2)_{\underline{3}}$, $(\bar{\psi}_L l_{2R})_{\underline{3}} (H \phi_l)_{\underline{3}}$ and $(\bar{\psi}_L l_{3R})_{\underline{3}} (H \phi_l^*)_{\underline{3}}$ which are responsible for generating masses for charged leptons as given in Eq. (20). The situation is similar for the remaining couplings that generate the mass matrices for neutrino sector. Besides, A_4 , Z_3 and Z_4 symmetries also prevent some interaction terms in the Higgs potential as discussed in Appendix A. It is well-known that 3+1 scheme-the minimal extended seesaw-by adding only one sterile neutrino ν_s cannot be anomaly free [56, 58], however, this may be solved by introducing additional fields required for anomaly cancelation [59] which is left for our future study.

⁵ The Lagrangian in Eq. (1) is performed with the additional symmetry Z_2 , where η_s and ν_s are even under Z_2 while all other fields are odd under Z_2 . This Z_2 symmetry ensures that the Γ invariant Yukawa term $\bar{\psi}_L \nu_s \tilde{H} \phi_s$ is absent from the Lagrangian.

It is interesting to note that, with the particle and scalar contents of the model in Table II, all the other quadratic terms forming a triplet under A_4 , including $(\phi_\nu\phi_\nu)_{3_s}$, $(\phi_\nu\phi_\nu)_{3_a}$, $(\phi_s\phi_s)_{3_s}$ and $(\phi_s\phi_s)_{3_a}$ can combine with H to form A_4 singlets but one cannot construct an invariant under Z_3 and/or Z_4 . Thus, the charged lepton mass expressions in our model (20) is much simpler compared to that of Ref. [55]. In fact, there exist the other contributions via higher dimensional Weinberg operators⁶ $\frac{1}{\Lambda^{2(k+l+1)}} \left(\bar{\psi}_L^c \psi_L \right)_1 H^2 \eta (H^\dagger H)^k (\eta^\dagger \eta)^l$ and $\frac{1}{\Lambda^{2(k+l)+3}} \left(\bar{\psi}_L^c \psi_L \right)_{3_s} H^2 (\eta \phi_\nu)_3 (H^\dagger H)^k (\eta^\dagger \eta)^l$, with $k, l = 0, 1, 2, \dots$. However, because $v_H \ll v_\eta, v_\nu \ll \Lambda$, the left-handed neutrinos generated by the Type-II seesaw mechanism, $\sim v_H \left(\frac{v_H}{\Lambda} \right)^{2k+1} \left(\frac{v_\eta}{\Lambda} \right)^{2l+1}$ and $v_H \left(\frac{v_H}{\Lambda} \right)^{2k+1} \left(\frac{v_\nu}{\Lambda} \right) \left(\frac{v_\eta}{\Lambda} \right)^{2l+1}$, are very small compared to the ones generated via the canonical type-I seesaw mechanism obtained in Eq. (26) and thus would be neglected in the Lagrangian (1).

The VEVs of scalar fields are chosen as follows

$$\begin{aligned} \langle H \rangle &= \begin{pmatrix} 0 \\ v_H \end{pmatrix}, \quad \langle \phi_\nu \rangle = (0 \ \langle \phi_{2\nu} \rangle \ 0), \quad \langle \phi_{2\nu} \rangle = v_\nu, \quad \langle \eta \rangle = v_\eta, \\ \langle \eta_s \rangle &= v_{\eta_s}, \quad \langle \phi_l \rangle = (\langle \phi_{1l} \rangle \ \langle \phi_{2l} \rangle \ \langle \phi_{3l} \rangle), \quad \langle \phi_{1l} \rangle = \langle \phi_{2l} \rangle = \langle \phi_{3l} \rangle = v_l, \\ \langle \phi_s \rangle &= (\langle \phi_{1s} \rangle \ \langle \phi_{2s} \rangle \ \langle \phi_{3s} \rangle), \quad \langle \phi_{1s} \rangle = \langle \phi_{3s} \rangle = v_s, \quad \langle \phi_{2s} \rangle = 0. \end{aligned} \quad (2)$$

The fact that the electroweak symmetry breaking scale is [84, 85]

$$v \sim 10^2 \text{ GeV}. \quad (3)$$

The scale of $B - L$ symmetry breaking is undetermined, spanning from TeV to much higher scales [86–89]. In this study, assume that the $B - L$ symmetry breaking is at TeV scale [86] while the cut-off scale⁷ is at a very high scale [55],

$$v_{\eta_s} \sim v_\eta \sim 10^3 \text{ GeV}, \quad \Lambda \sim 10^{13} \text{ GeV}. \quad (4)$$

On the other hand, the model result in Eq. (20) tells us that $\frac{m_e}{m_\mu} = \frac{2v_l}{\Lambda} \frac{x_{1cl}}{x_{3cl}} \sim \frac{v_l}{\Lambda}$, i.e., $\frac{m_e}{m_\mu} \sim \frac{v_l}{\Lambda}$ provided that $x_{1cl} \sim x_{3cl}$. Furthermore, the experimental data [108] implies that $\frac{m_e}{m_\mu} \sim 10^{-3}$. The VEV of singlets with $B - L = 0$ are assumed to be in the same scale, i.e., $v_l \sim v_\nu \sim v_s$. In this sense, we get the scale of VEVs of the flavons as follows:

$$v_l \sim v_\nu \sim v_s \sim 10^{10} \text{ GeV}. \quad (5)$$

⁶ Another operator $\frac{1}{\Lambda^{2(k+l)+3}} \left(\bar{\psi}_L^c \psi_L \right)_{3_a} H^2 (\eta \phi_\nu)_3 (H^\dagger H)^k (\eta^\dagger \eta)^l$ which is invariant under Γ but vanished due to the symmetric in $\bar{\psi}_{iL}^c$ and ψ_{jL} ($i, j = 1, 2, 3; i \neq j$).

⁷ In Ref. [90] the cut-off scale in the QED case is $\Lambda_{\text{EW}} \simeq 3.8 \times 10^{13} \text{ GeV}$; thus, we chose $\Lambda = 10^{13} \text{ GeV}$ for its scale.

From Eq. (1), with the help of Eqs. (3)-(5), after spontaneous symmetry breaking one can estimate the scales of the mass terms as follows:

$$\begin{aligned} \bar{l}_L l_{1R} &\sim \frac{v_H v_l^2}{\Lambda^2} \sim 10^{-4} \text{ GeV}, \quad \bar{l}_L l_{2R} \sim \bar{l}_L l_{3R} \sim \frac{v_H v_l}{\Lambda} \sim 10^{-1} \text{ GeV}, \\ \bar{\nu}_L \nu_R &\sim v_H \sim 10^2 \text{ GeV}, \quad \bar{\nu}_R^c \nu_R \sim v_\eta \sim 10^3 \text{ GeV}, \quad \bar{\nu}_s^c \nu_R \sim \frac{v_{\eta_s} v_s}{\Lambda} \sim 1 \text{ GeV}. \end{aligned} \quad (6)$$

III. SCALAR POTENTIAL MINIMUM CONDITION

In this section we will show that the VEV alignments in Eq. (2) satisfies the minimization condition of the scalar potential V_{scalar} in Appendix A. Indeed, in the minimization condition of V_{scalar} , we put $v_{\phi_{1l}} = v_{\phi_{2l}} = v_{\phi_{3l}} = v_l$, $v_{\phi_{1\nu}} = v_{\phi_{3\nu}} = 0$, $v_{\phi_{2\nu}} = v_\nu$, $v_{\phi_{2s}} = 0$, $v_{\phi_{1s}} = v_{\phi_{3s}} = v_s$ and $v_H^* = v_H$, $v_l^* = v_l$, $v_\nu^* = v_\nu$, $v_\eta^* = v_\eta$, $v_{\eta_s}^* = v_{\eta_s}$ and $v_s^* = v_s$ which leads to

$$\frac{\partial V_{\text{scalar}}}{\partial v_k^*} = \frac{\partial V_{\text{scalar}}}{\partial v_k}, \quad \frac{\partial^2 V_{\text{scalar}}}{\partial v_k^{*2}} = \frac{\partial^2 V_{\text{scalar}}}{\partial v_k^2} \quad (v_k = v_H, v_l, v_\nu, v_\eta, v_{\eta_s}, v_s), \quad (7)$$

and the scalar potential minimum condition reduces to

$$\mu_H^2 + 2\lambda^H v_H^2 + 3\lambda^{H\phi_l} v_l^2 + \lambda^{H\phi_\nu} v_\nu^2 + \lambda^{H\eta} v_\eta^2 + 2\lambda^{H\phi_s} v_s^2 + 2\Lambda^{H\phi_l\phi_\nu\phi_s} v_\nu + \lambda^{H\eta_s} v_{\eta_s}^2 = 0, \quad (8)$$

$$\begin{aligned} 3\mu_{\phi_l}^2 + 3\lambda^{H\phi_l} v_H^2 + 6\lambda^{\phi_l} v_l^2 + 3\lambda^{\phi_l\eta} v_\eta^2 + \lambda^{\phi_l\phi_\nu} v_\nu^2 + \lambda^{\phi_l\phi_s} v_s^2 + 2\Lambda_1^{H\phi_l\phi_\nu\eta\phi_s} v_\nu \\ + (3\lambda^{\phi_l\eta_s} + 2\lambda^{\phi_l\phi_\nu\eta_s} v_\nu) v_{\eta_s}^2 = 0, \end{aligned} \quad (9)$$

$$\begin{aligned} (\mu_{\phi_\nu}^2 + \lambda^{H\phi_\nu} v_H^2 + \lambda^{\phi_l\phi_\nu} v_l^2 + 2\lambda^{\phi_\nu} v_\nu^2 + \lambda^{\phi_\nu\eta} v_\eta^2 - \lambda^{\phi_\nu\phi_s} v_s^2) v_\nu + \Lambda_2^{H\phi_l\phi_\nu\eta\phi_s} v_l^2 \\ + \Lambda_3^{H\phi_l\phi_\nu\eta\phi_s} v_s^2 + v_{\eta_s}^2 (\lambda^{\phi_l\phi_\nu\eta_s} v_l^2 + \lambda^{\phi_\nu\eta_s} v_\nu + \lambda^{\phi_\nu\phi_s\eta_s} v_s^2) = 0, \end{aligned} \quad (10)$$

$$\mu_\eta^2 + \lambda^{H\eta} v_H^2 + 3\lambda^{\phi_l\eta} v_l^2 + \lambda^{\phi_\nu\eta} v_\nu^2 + 2\lambda^\eta v_\eta^2 + 2\lambda^{\phi_s\eta} v_s^2 + 2\Lambda^{\phi_l\phi_\nu\eta\phi_s} v_\nu + \lambda^{\eta\eta_s} v_{\eta_s}^2 = 0, \quad (11)$$

$$\begin{aligned} 2\mu_s^2 + 2\lambda^{H\phi_s} v_H^2 + \lambda^{\phi_l\phi_s} v_l^2 - \lambda^{\phi_\nu\phi_s} v_\nu^2 + 2\lambda^{\phi_s\eta} v_\eta^2 + 2\lambda^{\phi_s} v_s^2 + 2\Lambda_3^{H\phi_l\phi_\nu\eta\phi_s} v_\nu \\ + 2(\lambda^{\phi_s\eta_s} + \lambda^{\phi_l\phi_s\eta_s} v_\nu) v_{\eta_s}^2 = 0, \end{aligned} \quad (12)$$

$$\begin{aligned} \mu_{\eta_s}^2 + \lambda^{\eta\eta_s} v_\eta^2 + 2\lambda^{\eta_s} v_{\eta_s}^2 + \lambda^{H\eta_s} v_H^2 + 3\lambda^{\phi_l\eta_s} v_l^2 + \lambda^{\phi_\nu\eta_s} v_\nu^2 + 2\lambda^{\phi_s\eta_s} v_s^2 \\ + 2(\lambda^{\phi_l\phi_\nu\eta_s} v_l^2 + \lambda^{\phi_\nu\phi_s\eta_s} v_s^2) v_\nu = 0, \end{aligned} \quad (13)$$

$$\lambda^H v_H > 0, \quad \lambda^{\phi_l} v_l > 0, \quad \lambda^\eta v_\eta > 0, \quad \lambda^{\phi_s} v_s > 0, \quad \lambda^{\eta_s} v_{\eta_s} > 0, \quad (14)$$

$$\mu_\nu^2 + \lambda^{\phi_\nu\eta} v_\eta^2 + \lambda^{H\phi_\nu} v_H^2 + \lambda^{\phi_l\phi_\nu} v_l^2 + 6\lambda^{\phi_\nu} v_\nu^2 - \lambda^{\phi_\nu\phi_s} v_s^2 + \lambda^{\phi_\nu\eta_s} v_{\eta_s}^2 > 0, \quad (15)$$

where, the following notations have been introduced:

$$\begin{aligned}
\Lambda^{H\phi_l\phi_\nu\phi_s} &= \lambda_1^{H\phi_l\phi_s} v_l^2 + \lambda_1^{H\phi_s\phi_\nu} v_s^2, \quad \Lambda^{\phi_l\phi_\nu\eta\phi_s} = \lambda_1^{\phi_l\phi_\nu\eta} v_l^2 + \lambda_1^{\phi_\nu\eta\phi_s} v_s^2, \\
\Lambda_1^{H\phi_l\phi_\nu\eta\phi_s} &= \lambda_1^{\phi_l\phi_\nu\eta} v_\eta^2 + \lambda_1^{H\phi_l\phi_s} v_H^2 + \lambda^{\phi_l\phi_\nu\phi_s} v_s^2, \quad \Lambda_2^{H\phi_l\phi_\nu\eta\phi_s} = \lambda_1^{\phi_l\phi_\nu\eta} v_\eta^2 + \lambda_1^{H\phi_l\phi_s} v_H^2, \\
\Lambda_3^{H\phi_l\phi_\nu\eta\phi_s} &= \lambda_1^{\phi_\nu\eta\phi_s} v_\eta^2 + \lambda_1^{H\phi_s\phi_\nu} v_H^2 + \lambda^{\phi_l\phi_\nu\phi_s} v_l^2, \\
\lambda^{H\eta} &= \lambda_1^{H\eta} + \lambda_2^{H\eta}, \quad \lambda^{H\phi_l} = \lambda_1^{H\phi_l} + \lambda_2^{H\phi_l}, \quad \lambda^{H\phi_\nu} = \lambda_1^{H\phi_\nu} + \lambda_2^{H\phi_\nu}, \\
\lambda^{H\phi_s} &= \lambda_1^{H\phi_s} + \lambda_2^{H\phi_s}, \quad \lambda^{\phi_l\eta} = \lambda_1^{\phi_l\eta} + \lambda_2^{\phi_l\eta}, \quad \lambda^{\phi_s\eta} = \lambda_1^{\phi_s\eta} + \lambda_2^{\phi_s\eta}, \\
\lambda^{H\phi_l} &= \lambda_1^{H\phi_l} + \lambda_2^{H\phi_l}, \quad \lambda^{\phi_l} = 3\lambda_1^{\phi_l} + 4\lambda_4^{\phi_l}, \\
\lambda^{\phi_l\phi_\nu} &= 3\lambda_1^{\phi_l\phi_\nu} + \lambda_6^{\phi_l\phi_\nu} + \lambda_7^{\phi_l\phi_\nu} + \lambda_8^{\phi_l\phi_\nu} + 2\lambda_9^{\phi_l\phi_\nu} - 2\lambda_{10}^{\phi_l\phi_\nu}, \\
\lambda^{\phi_l\phi_s} &= 6\lambda_1^{\phi_l\phi_s} + 4\lambda_4^{\phi_l\phi_s} + 4\lambda_6^{\phi_l\phi_s} + \lambda_7^{\phi_l\phi_s} + \lambda_8^{\phi_l\phi_s} + 6\lambda_9^{\phi_l\phi_s} - 2\lambda_{10}^{\phi_l\phi_s}, \\
\lambda^{\phi_\nu\phi_s} &= -2\lambda_1^{\phi_\nu\phi_s} + \lambda_2^{\phi_\nu\phi_s} + \lambda_3^{\phi_\nu\phi_s} - 2\lambda_9^{\phi_\nu\phi_s} + 2\lambda_{10}^{\phi_\nu\phi_s}, \\
\lambda^{\phi_\nu\eta} &= \lambda_1^{\phi_\nu\eta} + \lambda_2^{\phi_\nu\eta}, \quad \lambda^{\phi_\nu} = \lambda_1^{\phi_\nu} + \lambda_2^{\phi_\nu} + \lambda_3^{\phi_\nu}, \quad \lambda^{\phi_s} = \lambda_2^{\phi_s} + \lambda_3^{\phi_s} + 4(\lambda_1^{\phi_s} + \lambda_4^{\phi_s}), \\
\lambda^{\phi_l\phi_\nu\phi_s} &= 2\lambda_1^{\phi_l\phi_\nu\phi_s} + 3\lambda_3^{\phi_l\phi_\nu\phi_s} + 2(\lambda_5^{\phi_l\phi_\nu\phi_s} + \lambda_7^{\phi_l\phi_\nu\phi_s}), \\
\lambda^{H\eta_s} &= \lambda_1^{H\eta_s} + \lambda_2^{H\eta_s}, \quad \lambda^{\phi_l\eta_s} = \lambda_1^{\phi_l\eta_s} + \lambda_2^{\phi_l\eta_s}, \quad \lambda^{\phi_\nu\eta_s} = \lambda_1^{\phi_\nu\eta_s} + \lambda_2^{\phi_\nu\eta_s}, \\
\lambda^{\eta\eta_s} &= \lambda_1^{\eta\eta_s} + \lambda_2^{\eta\eta_s}, \quad \lambda^{\phi_s\eta_s} = \lambda_1^{\phi_s\eta_s} + \lambda_2^{\phi_s\eta_s}.
\end{aligned} \tag{17}$$

Assuming that μ_H , μ_{ϕ_l} , μ_{ϕ_ν} , μ_η and μ_s are negative and of the same order of magnitude as that of the SM [108]⁸,

$$\mu_H^2 = \mu_{\phi_l}^2 = \mu_{\phi_\nu}^2 = \mu_\eta^2 = \mu_{\eta_s}^2 = \mu_s^2 = -10^4 \text{ GeV}. \tag{18}$$

Using (3)-(5), (18) and the following benchmark point

$$\begin{aligned}
\lambda^{H\phi_l} &= \lambda^{H\phi_\nu} = \lambda^{H\eta} = \lambda^{H\phi_s} = \lambda^{\phi_l\phi_\nu} = \lambda^{\phi_l\eta} = \lambda^{\phi_l\phi_s} = \lambda^{\phi_\nu\eta} \\
&= \lambda^{\phi_\nu\phi_s} = \lambda^{\phi_s\eta} = \lambda^{H\eta_s} = \lambda^{\phi_l\eta_s} = \lambda^{\phi_\nu\eta_s} = \lambda^{\eta\eta_s} = \lambda^{\phi_s\eta_s} = \lambda^x, \\
\lambda^{\phi_l\phi_\nu\phi_s} &= \lambda_1^{H\phi_l\phi_s} = \lambda_1^{\phi_l\phi_\nu\eta} = \lambda_1^{\phi_\nu\eta\phi_s} = \lambda_1^{H\phi_s\phi_\nu} = \lambda^{\phi_l\phi_\nu\eta_s} = \lambda^{\phi_l\phi_s\eta_s} = \lambda^y,
\end{aligned} \tag{19}$$

the quantities $\frac{\partial^2 V_{\text{scalar}}}{\partial \langle \Phi \rangle^2}$ ($\Phi = H, \phi_l, \phi_\nu, \eta, \phi_s, \eta_s$) depend on two parameters λ^x and λ^y with $\lambda^x \in (-10^{-2}, -10^{-3})$ and $\lambda^y \in (-10^{-3}, -10^{-4})$. Fig.1 implies that⁹, the inequalities in (14) and (15) are always satisfied by the solutions of Eqs. (8)–(12) as given in Appendix B. This proves that the VEV alignments in Eq. (2) is the natural solution of the minimum condition of V_{scalar} as expected.

⁸ In th SM [108], $|\mu| = 88.4$ GeV; thus, we use $|\mu_H| \sim |\mu_\phi| \sim |\mu_l| \sim |\mu_\nu| \sim |\mu_s| = 10^2$ GeV for their scales.

⁹ As an example, in the case of $\lambda^x = -10^{-3}$ and $\lambda^y = -10^{-4}$ we get $\frac{\partial^2 V_{\text{scalar}}}{\partial \langle H \rangle^2} \sim 10^{43}$, $\frac{\partial^2 V_{\text{scalar}}}{\partial \langle \phi_l \rangle^2} \sim \frac{\partial^2 V_{\text{scalar}}}{\partial \langle \phi_s \rangle^2} \sim 10^{34}$, $\frac{\partial^2 V_{\text{scalar}}}{\partial \langle \phi_\nu \rangle^2} \sim 10^{53}$ and $\frac{\partial^2 V_{\text{scalar}}}{\partial \langle \eta \rangle^2} \sim \frac{\partial^2 V_{\text{scalar}}}{\partial \langle \eta_s \rangle^2} \sim 10^{42}$.

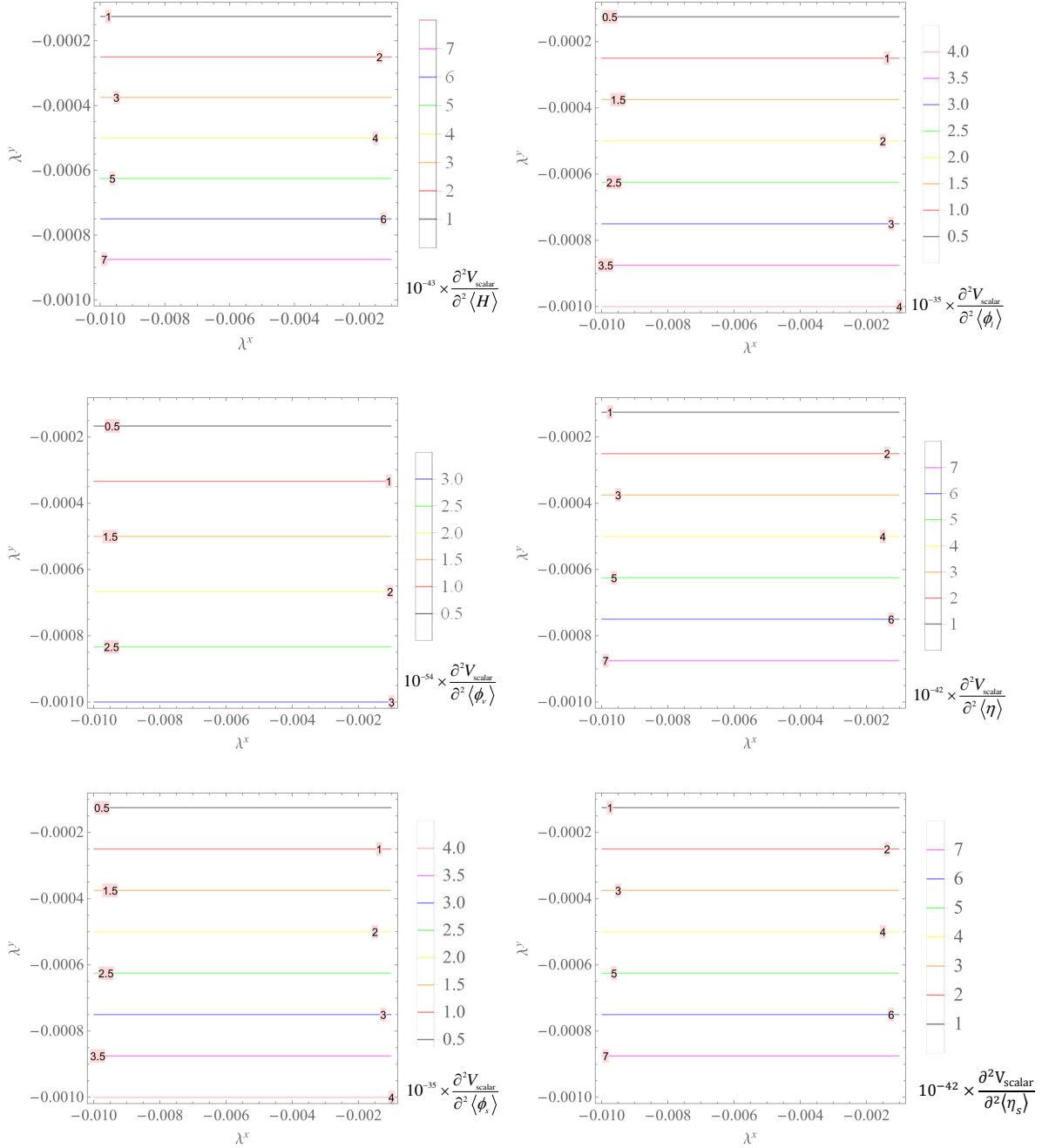


Figure 1. $\frac{\partial^2 V_{\text{scalar}}}{\partial \langle \Phi \rangle^2}$ ($\Phi = H, \phi_l, \phi_\nu, \eta, \phi_s, \eta_s$) versus λ^x and λ^y with $\lambda^x \in (-10^{-2}, -10^{-3})$ and $\lambda^y \in (-10^{-3}, -10^{-4})$.

IV. 3+1 ACTIVE - STERILE NEUTRINO MIXING

With the help of (2) and the Clebsch-Gordan coefficients of A_4 group [107], from Eq. (1) we get the charged lepton masses and the corresponding mixing matrices:

$$m_e = 2\sqrt{3}x_{1cl}v_H \left(\frac{v_l}{\Lambda}\right)^2, \quad m_\mu = \sqrt{3}x_{2cl}v_H \frac{v_l}{\Lambda}, \quad m_\tau = \sqrt{3}v_H x_{3cl} \frac{v_l}{\Lambda}, \quad (20)$$

$$U_L^+ = \frac{1}{\sqrt{3}} \begin{pmatrix} 1 & 1 & 1 \\ 1 & \omega^2 & \omega \\ 1 & \omega & \omega^2 \end{pmatrix}, \quad U_R = 1, \quad \omega = e^{i2\pi/3}. \quad (21)$$

The Eq. (20) tells us that m_e is suppressed by a factor of $v_H \left(\frac{v_l}{\Lambda}\right)^2 \sim 10^{-4}$ GeV compared to m_μ and m_τ of the order of $\frac{v_H v_l}{\Lambda} \sim 10^{-1}$ GeV. Thus, the considered model naturally explain the charged-lepton mass hierarchy.

By comparing $m_{e,\mu,\tau}$ in (20) with the data given in Ref. [108], $m_e \simeq 0.511$ MeV, $m_\mu \simeq 105.66$ MeV and $m_\tau \simeq 1776.86$ MeV, along with the help of Eqs. (3)-(5), we obtain

$$x_{1cl} = 0.848, \quad x_{2cl} = 0.351, \quad x_{3cl} = 5.90. \quad (22)$$

Coming back to the neutrino sector. Using the Clebsch-Gordan coefficient property of A_4 group [107], from Eq. (1), the Lagrangian for the neutrino sector becomes

$$\begin{aligned} -\mathcal{L}_\nu = & x_{1\nu} (\bar{\psi}_{1L}\nu_{1R} + \bar{\psi}_{2L}\nu_{2R} + \bar{\psi}_{3L}\nu_{3R}) \tilde{H} \\ & + \frac{x_{2\nu}}{\Lambda} \left[(\bar{\psi}_{2L}\nu_{3R} + \bar{\psi}_{3L}\nu_{2R}) \tilde{H} \phi_{1\nu} + (\bar{\psi}_{3L}\nu_{1R} + \bar{\psi}_{1L}\nu_{3R}) \tilde{H} \phi_{2\nu} + (\bar{\psi}_{1L}\nu_{2R} + \bar{\psi}_{2L}\nu_{1R}) \tilde{H} \phi_{3\nu} \right] \\ & + \frac{x_{3\nu}}{\Lambda} \left[(\bar{\psi}_{2L}\nu_{3R} - \bar{\psi}_{3L}\nu_{2R}) \tilde{H} \phi_{1\nu} + (\bar{\psi}_{3L}\nu_{1R} - \bar{\psi}_{1L}\nu_{3R}) \tilde{H} \phi_{2\nu} + (\bar{\psi}_{1L}\nu_{2R} - \bar{\psi}_{2L}\nu_{1R}) \tilde{H} \phi_{3\nu} \right] \\ & + \frac{y_\nu}{2} (\bar{\nu}_{1R}^c \nu_{1R} + \bar{\nu}_{2R}^c \nu_{2R} + \bar{\nu}_{2R}^c \nu_{3R}) \eta + \frac{y_s}{\Lambda} (\bar{\nu}_s^c \nu_{1R} \eta_{\textcolor{blue}{S}} \phi_{1s} + \bar{\nu}_s^c \nu_{2R} \eta_{\textcolor{blue}{S}} \phi_{2s} + \bar{\nu}_s^c \nu_{3R} \eta_{\textcolor{blue}{S}} \phi_{3s}) \\ & + \text{H.c.} \end{aligned} \quad (23)$$

After symmetry breaking, we find the 7×7 neutrino mass matrix in the basis (ν_L, ν_R^c, S^c) as follows

$$M_\nu^{7 \times 7} = \begin{pmatrix} 0 & M_D & 0 \\ M_D^T & M_R & M_S^T \\ 0 & M_S & 0 \end{pmatrix}, \quad (24)$$

where M_D , M_R and M_S take the form:

$$\begin{aligned} M_D = v_H & \begin{pmatrix} x_{1\nu} & 0 & \frac{v_\nu}{\Lambda} (x_{2\nu} - x_{3\nu}) \\ 0 & x_{1\nu} & 0 \\ \frac{v_\nu}{\Lambda} (x_{2\nu} + x_{3\nu}) & 0 & x_{1\nu} \end{pmatrix}, \\ M_R = y_\nu v_\eta \mathbf{I}, \quad M_S = & \frac{y_s}{\Lambda} v_{\eta_{\textcolor{blue}{S}}} v_s (1 \quad 0 \quad 1). \end{aligned} \quad (25)$$

In the case where $M_R \gg M_S > M_D$, the effective 4×4 light neutrino mass matrix in the basis (ν_L, S^c) is constructed by the following expression [55, 56, 58, 60]:

$$M_\nu = - \begin{pmatrix} M_D M_R^{-1} M_D^T & M_D M_R^{-1} M_S^T \\ M_S (M_R^{-1})^T M_D^T & M_S M_R^{-1} M_S^T \end{pmatrix}. \quad (26)$$

The expression (25) shows that, there are five complex parameters thus has ten real parameters in the neutrino sector. Considering the case of real VEV for the singlet scalars ϕ_ν , ϕ_s and η , the phase redefinition of the leptonic fields ψ_L , ν_R and ν_s allows to rotate away the phase of four neutrino Yukawa couplings $x_{2\nu}$, $x_{3\nu}$, y_ν and y_s , reducing to six physical parameters. On the other hand, one parameter is absorbed by defining the hermitian matrix. Thus, in the neutrino sector, there are five real parameters, including $\alpha_1 = \arg(x_{1\nu})$, $k_{2,3}$, m_0 and m_s which are defined are defined as follows:

$$k_2 = \frac{v_\nu x_{2\nu}}{\Lambda |x_{1\nu}|}, \quad k_3 = \frac{v_\nu x_{3\nu}}{\Lambda |x_{1\nu}|}, \quad m_0 = \frac{v_H^2 |x_{1\nu}|^2}{v_\eta y_\nu}, \quad m_s = \frac{2v_{\eta_s}^2 v_s^2 y_s^2}{v_\eta \Lambda^2 y_\nu}. \quad (27)$$

Combining Eqs.(25) and (26) yields:

$$M_\nu^{4 \times 4} = - \begin{pmatrix} m_0 \begin{pmatrix} e^{2i\alpha_1} + (k_2 - k_3)^2 & 0 & 2k_2 e^{i\alpha_1} \\ 0 & e^{2i\alpha_1} & 0 \\ 2k_2 e^{i\alpha_1} & 0 & e^{2i\alpha_1} + (k_2 + k_3)^2 \end{pmatrix} \sqrt{\frac{m_0 m_s}{2}} \begin{pmatrix} e^{i\alpha_1} + (k_2 - k_3) \\ 0 \\ e^{i\alpha_1} + (k_2 + k_3) \end{pmatrix} \\ \sqrt{\frac{m_0 m_s}{2}} \begin{pmatrix} e^{i\alpha_1} + (k_2 - k_3) & 0 & e^{i\alpha_1} + (k_2 + k_3) \end{pmatrix} & m_s \end{pmatrix}, \quad (28)$$

where $\alpha_1 = \arg(x_{1\nu})$, and $k_{2,3}$, m_0 and m_s are defined in Eq. (27).

Suppose that $M_D < M_s$, we can therefore apply the type-I seesaw mechanism on Eq.(26) to obtain the active neutrino mass matrix as [55, 56, 58, 60]

$$\begin{aligned} M_\nu &= M_D M_R^{-1} M_s^T (M_s M_R^{-1} M_s^T)^{-1} M_s M_R^{-1} M_D^T - M_D M_R^{-1} M_D^T \\ &= -\frac{m_0}{2} \begin{pmatrix} (e^{i\alpha_1} - (k_2 - k_3))^2 & 0 & k_3^2 - (e^{i\alpha_1} - k_2)^2 \\ 0 & 2e^{2i\alpha_1} & 0 \\ k_3^2 - (e^{i\alpha_1} - k_2)^2 & 0 & (e^{i\alpha_1} - (k_2 + k_3))^2 \end{pmatrix}. \end{aligned} \quad (29)$$

Since $k_{2,3}$ and m_0 are real, M_ν is complex. To diagonalise the matrix M_ν , let us define a Hermitian matrix \mathbf{m}_ν^2 , given by

$$\mathbf{m}_\nu^2 = M_\nu M_\nu^\dagger = \frac{m_0^2}{2} \begin{pmatrix} A_1 + A_2 & 0 & -B_1 + iB_2 \\ 0 & 2 & 0 \\ -B_1 - iB_2 & 0 & A_1 - A_2 \end{pmatrix}, \quad (30)$$

where

$$\begin{aligned} A_1 &= (1 + k_2^2 + k_3^2 - 2k_2 \cos \alpha_1)^2, \\ A_2 &= 2k_3(\cos \alpha_1 - k_2)(1 + k_2^2 + k_3^2 - 2k_2 \cos \alpha_1), \\ B_1 &= (1 + k_2^2 - k_3^2 - 2k_2 \cos \alpha_1)(1 + k_2^2 + k_3^2 - 2k_2 \cos \alpha_1), \\ B_2 &= 2k_3(1 + k_2^2 + k_3^2 - 2k_2 \cos \alpha_1) \sin \alpha_1. \end{aligned} \quad (31)$$

The matrix \mathbf{m}_ν^2 in Eq. (30) is diagonalized by U_ν satisfying

$$U_\nu^+ \mathbf{m}_\nu^2 U_\nu = \begin{cases} \begin{pmatrix} 0 & 0 & 0 \\ 0 & m_0^2 & 0 \\ 0 & 0 & k_0^2 m_0^2 \end{pmatrix}, & U_\nu = \begin{pmatrix} \frac{1}{x_1+ix_2} & 0 & -\frac{1}{y_1+iy_2} \\ 0 & 1 & 0 \\ \frac{1}{x_0} & 0 & \frac{1}{y_0} \end{pmatrix} \text{ for NH,} \\ \begin{pmatrix} k_0^2 m_0^2 & 0 & 0 \\ 0 & m_0^2 & 0 \\ 0 & 0 & 0 \end{pmatrix}, & U_\nu = \begin{pmatrix} -\frac{1}{y_1+iy_2} & 0 & \frac{1}{x_1+ix_2} \\ 0 & 1 & 0 \\ \frac{1}{y_0} & 0 & \frac{1}{x_0} \end{pmatrix} \text{ for IH,} \end{cases} \quad (32)$$

thus the light neutrino masses are

$$\begin{cases} m_1^2 = 0, & m_2^2 = m_0^2, m_3^2 = m_0^2 k_0^2 \text{ for NH,} \\ m_1^2 = m_0^2 k_0^2, & m_2^2 = m_0^2, m_3^2 = 0 \text{ for IH,} \end{cases} \quad (33)$$

where

$$k_0 = 1 + k_2^2 + k_3^2 - 2k_2 \cos \alpha_1, \quad (34)$$

$$x_0 = \sqrt{\frac{2k_0}{k_0 + 2k_3(\cos \alpha_1 - k_2)}}, \quad y_0 = \sqrt{\frac{2k_0}{k_0 + 2k_3(k_2 - \cos \alpha_1)}}, \quad (35)$$

$$x_1 = \frac{(k_0 - 2k_3^2)x_0}{k_0 + 2k_3(k_2 - \cos \alpha_1)}, \quad y_1 = \frac{(k_0 - 2k_3^2)y_0}{k_0 + 2k_3(\cos \alpha_1 - k_2)}, \quad (36)$$

$$x_2 = \frac{2k_3 x_0 \sin \alpha_1}{k_0 + 2k_3(k_2 - \cos \alpha_1)}, \quad y_2 = \frac{2k_3 y_0 \sin \alpha_1}{k_0 + 2k_3(\cos \alpha_1 - k_2)}. \quad (37)$$

The corresponding leptonic mixing matrix is

$$U_{lep} = U_L^\dagger U_\nu = \begin{cases} \frac{1}{\sqrt{3}} \begin{pmatrix} \frac{1}{x_0} + \frac{1}{x_1+ix_2} & 1 & \frac{1}{y_0} - \frac{1}{y_1+iy_2} \\ \frac{\omega}{x_0} + \frac{1}{x_1+ix_2} & \omega^2 & \frac{\omega}{y_0} - \frac{1}{y_1+iy_2} \\ \frac{\omega^2}{x_0} + \frac{1}{x_1+ix_2} & \omega & \frac{\omega^2}{y_0} - \frac{1}{y_1+iy_2} \end{pmatrix} & \text{for NH,} \\ \frac{1}{\sqrt{3}} \begin{pmatrix} \frac{1}{y_0} - \frac{1}{y_1+iy_2} & 1 & \frac{1}{x_0} + \frac{1}{x_1+ix_2} \\ \frac{\omega}{y_0} - \frac{1}{y_1+iy_2} & \omega^2 & \frac{\omega}{x_0} + \frac{1}{x_1+ix_2} \\ \frac{\omega^2}{y_0} - \frac{1}{y_1+iy_2} & \omega & \frac{\omega^2}{x_0} + \frac{1}{x_1+ix_2} \end{pmatrix} & \text{for IH,} \end{cases} \quad (38)$$

which being being the TM_2 form. Eq. (33) implies the neutrino mass ordering should be either $(0, m_0, m_0 k_0)$ or $(m_0 k_0, m_0, 0)$. It is very interesting to note that depending on the sign of $\cos \alpha_1$, k_0 can be greater or less than 1 so both NH ($m_1 < m_2$) and IH ($m_2 < m_1$) are consistent with the experimental data given that k_2 and k_3 are real parameters. Therefore, our model predicts both NH and IH of the active neutrino masses which is in consistent with the data taken from Ref. [1] and different from that of Ref. [55].

The lepton mixing angles, in the three-neutrino scheme, is defined as [108]

$$s_{13}^2 = |\mathbf{U}_{e3}|^2 = \begin{cases} \frac{2}{3} \frac{k_3^2}{k_0} & \text{for NH,} \\ \frac{2}{3} \left(1 - \frac{k_3^2}{k_0}\right) & \text{for IH,} \end{cases} \quad (39)$$

$$s_{12}^2 = \frac{|\mathbf{U}_{e2}|^2}{1 - |\mathbf{U}_{e3}|^2} = \frac{1}{3c_{13}^2} \quad \text{for both NH and IH,} \quad (40)$$

$$s_{23}^2 = \frac{|\mathbf{U}_{\mu 3}|^2}{1 - |\mathbf{U}_{e3}|^2} = \begin{cases} \frac{1}{2} + \frac{\sqrt{3}k_3 \sin \alpha_1}{3k_0 - 2k_3^2} & \text{for NH,} \\ \frac{1}{2} - \frac{\sqrt{3}k_3 \sin \alpha_1}{k_0 + 2k_3^2} & \text{for IH,} \end{cases} \quad (41)$$

where θ_{ij} are neutrino mixing angles and $t_{12} = s_{12}/c_{12}$, $t_{23} = s_{23}/c_{23}$, $c_{ij} = \cos \theta_{ij}$, $s_{ij} = \sin \theta_{ij}$.

The Jarlskog invariant, determined from Eq. (38), takes the form [108–111]

$$J_{CP} = \text{Im}(U_{12}U_{23}U_{13}^*U_{22}^*) = \begin{cases} \frac{k_3(\cos \alpha_1 - k_2)}{3\sqrt{3}k_0} & \text{for NH,} \\ \frac{k_3(k_2 - \cos \alpha_1)}{3\sqrt{3}k_0} & \text{for IH.} \end{cases} \quad (42)$$

From Eqs. (32) and (39)–(42), we can express m_0 , k_0 , $k_{2,3}$ and $\sin \delta_{CP}$ in terms of four observables Δm_{21}^2 , Δm_{31}^2 , s_{23}^2 and s_{13}^2 and α_1 as follows:

$$m_0^2 = \begin{cases} \Delta m_{21}^2 & \text{for NH,} \\ \Delta m_{21}^2 - \Delta m_{31}^2 & \text{for IH,} \end{cases} \quad (43)$$

$$k_0^2 = \begin{cases} \frac{\Delta m_{31}^2}{m_0^2} & \text{for NH,} \\ \frac{-\Delta m_{31}^2}{m_0^2} & \text{for IH,} \end{cases} \quad (44)$$

$$k_2 = \cos \alpha_1 \mp \sqrt{k_0 - k_3^2 - \sin^2 \alpha_1} \quad \text{for both NH and IH,} \quad (45)$$

$$k_3^2 = \begin{cases} \frac{3}{2} k_0 s_{13}^2 & \text{for NH,} \\ \frac{k_0}{2} (2 - 3s_{13}^2) & \text{for IH,} \end{cases} \quad (46)$$

$$\sin \delta_{CP} = \frac{3J_{CP}}{s_{13}s_{23}c_{23}\sqrt{2 - 3s_{13}^2}} \quad \text{for both NH and IH,} \quad (47)$$

with J_{CP} is determined in Eq. (42).

Using the approximation $M_D < M_s$, we obtain the mass of the 4th mass eigenstate [55, 56, 58, 60],

$$m_4 = -M_s M_R^{-1} M_s^T = m_s, \quad (48)$$

with m_s is defined in Eq. (27). Combining Eqs. (33) and (48) yields:

$$m_s = m_4 = \begin{cases} \sqrt{\Delta m_{41}^2} & \text{for NH,} \\ \sqrt{\Delta m_{41}^2 + m_0^2 k_0^2} & \text{for IH.} \end{cases} \quad (49)$$

The 4×4 light neutrino mixing matrix is given by [55, 56, 58, 60]:

$$U = U_L^\dagger U_\nu = \begin{pmatrix} U_L^\dagger (1 - \frac{1}{2} R R^\dagger) U_\nu & U_L^\dagger R \\ -R^\dagger U_\nu & 1 - \frac{1}{2} R^\dagger R \end{pmatrix}, \quad (50)$$

where the three-component column vector R is given by [55, 56, 58, 60]

$$R = M_D M_R^{-1} M_s^T (M_s M_R^{-1} M_s^T)^{-1} = \sqrt{\frac{m_0}{2m_s}} \begin{pmatrix} e^{i\alpha_1} + (k_2 - k_3) \\ 0 \\ e^{i\alpha_1} + (k_2 + k_3) \end{pmatrix}. \quad (51)$$

Combining Eqs. (21) and (51), the strength of the active-sterile mixing is given by

$$U_L^\dagger R = \frac{1}{\sqrt{6}} \sqrt{\frac{m_0}{m_s}} \begin{pmatrix} 2(e^{i\alpha_1} + k_2) \\ \frac{1}{2} [(1 - i\sqrt{3})(k_2 + e^{i\alpha_1}) - (3 + i\sqrt{3})k_3] \\ \frac{1}{2} [(1 + i\sqrt{3})(k_2 + e^{i\alpha_1}) - (3 - i\sqrt{3})k_3] \end{pmatrix} \equiv \begin{pmatrix} U_{e4} \\ U_{\mu 4} \\ U_{\tau 4} \end{pmatrix}, \quad (52)$$

which leads to

$$|U_{14}|^2 = \frac{2}{3} \frac{m_0}{m_s} (1 + k_2^2 + 2k_2 \cos \alpha_1), \quad (53)$$

$$|U_{24}|^2 = \frac{1}{6} \frac{m_0}{m_s} (1 + k_2^2 + 3k_3^2 + 2k_2 \cos \alpha_1 - 2\sqrt{3}k_3 \sin \alpha_1), \quad (54)$$

$$|U_{34}|^2 = \frac{1}{6} \frac{m_0}{m_s} (1 + k_2^2 + 3k_3^2 + 2k_2 \cos \alpha_1 + 2\sqrt{3}k_3 \sin \alpha_1). \quad (55)$$

The effective neutrino masses [112–114], determined from Eqs. (33), (38), (48) and (52), possess the following forms¹⁰:

$$\langle m_{ee} \rangle = \left| \sum_{i=1}^4 U_{ei}^2 m_i \right| = \frac{m_0}{3} \sqrt{\frac{\Gamma_e}{k_0 + 2k_3(k_2 - 2 \cos \alpha_1)}}, \quad (56)$$

$$m_\beta = \sqrt{\sum_{i=1}^4 |U_{ei}|^2 m_i^2} = \frac{m_0}{\sqrt{3}} \sqrt{1 + 2k_0 k_3^2 + \frac{2m_s}{m_0} (1 + k_2^2 + 2k_2 \cos \alpha_1)}, \quad (57)$$

$$\langle m_{ee}^{(3\nu)} \rangle = \left| \sum_{i=1}^3 U_{ei}^2 m_i \right| = \frac{m_0}{3} \sqrt{\frac{\Gamma_e^{(3)}}{k_0 + 2k_3(k_2 - 2 \cos \alpha_1)}}, \quad (58)$$

$$m_\beta^{(3\nu)} = \sqrt{\sum_{i=1}^3 |U_{ei}|^2 m_i^2} = \frac{m_0}{\sqrt{3}} \sqrt{1 + 2k_0 k_3^2}, \quad (59)$$

¹⁰ Eqs. (56) and (57) are satisfied for both NH and IH.

with

$$\begin{aligned}
\Gamma_e = & 5 + (1 + 8k_2^2 + 4k_2^4)k_2^2 + 2[4k_2^2(3 + k_2^2) - 7]k_2k_3 + [12(2 + k_2^2)k_2^2 + 5]k_3^2 \\
& + 8(2k_2^2 + 1)k_2k_3^3 + 4(3k_2^2 + 2)k_3^4 + 4(2k_2 + k_3)k_3^5 + 2[4(k_2^3 + 3k_2^2k_3 + 2k_3^3)k_2^2 \\
& - 7k_3 + (8k_3^2 - 4)k_2^3 + (5 + 8k_3^2 + 4k_3^4)k_2 - 4(1 + k_3^2)k_3^3] \cos \alpha_1 \\
& - 4[(2k_2^4 - 1) + (3 + 2k_3^2)k_2^2 + 4(1 + k_3^2)k_2k_3 - 2(1 + k_3^2)k_3^2] \cos 2\alpha_1 \\
& - 4[(1 + 2k_2^2)(k_2 + k_3) + 4k_3^3] \cos 3\alpha_1 + 8k_3^2 \cos 4\alpha_1, \tag{60}
\end{aligned}$$

$$\Gamma_e^{(3)} = 1 + 4k_3^2(k_3^2 + \cos 2\alpha_1) + (1 + 2k_3^2)^2[(k_2 + k_3)^2 - 2(k_2 + k_3) \cos \alpha_1]. \tag{61}$$

Although the NH seems favored by some global analysis[115–117], however, it is the fact that the neutrino mass spectrum is currently unknown and it can be normal ($m_1 < m_2 < m_3$) or inverted ($m_3 < m_1 < m_2$) ordering depending on the sign of Δm_{31}^2 [1, 118]. In the next section, we will show that our model can explain the sterile-active neutrino mass and mixing as well as the recent three neutrino oscillation data given in Table I in the minimal extended seesaw framework for both NH and IH.

V. NUMERICAL ANALYSIS

In this work, eleven independent experimentally measured quantities in the neutrino sector, including $\sin^2 \theta_{12}$, $\sin^2 \theta_{23}$, $\sin^2 \theta_{13}$, $\sin \delta$, Δm_{21}^2 , Δm_{31}^2 , $\langle m_{ee} \rangle$, Δm_{41}^2 , $|U_{14}|^2$, $|U_{24}|^2$ and $|U_{34}|^2$, can be expressed in terms of five model parameters including k_2 , k_3 , m_0 , m_s and α_1 . We calculate the model parameters using the experimental data and also make predictions. To calculate the allowed ranges of the model parameters k_2 , k_3 , m_0 , m_s and α_1 as well as predictive ranges for the experimental parameters $\sin^2 \theta_{12}$, $\sin \delta$, $\langle m_{ee} \rangle$, $|U_{14}|^2$, $|U_{24}|^2$ and $|U_{34}|^2$, we utilize the observables Δm_{21}^2 , Δm_{31}^2 , Δm_{41}^2 , $\sin^2 \theta_{13}$ and $\sin^2 \theta_{23}$ whose experimental values are shown in Table I.

Firstly, using the 3σ experimental range of Δm_{21}^2 and Δm_{31}^2 taken from Tab. I, we get the constraints

$$m_0^2 \in \begin{cases} (69.4, 81.4) \text{ meV}^2 & \text{for NH,} \\ (2439, 2611) \text{ meV}^2 & \text{for IH,} \end{cases} \tag{62}$$

$$k_0^2 \in \begin{cases} (30.34, 37.90) \text{ meV} & \text{for NH,} \\ (0.967, 0.973) \text{ meV} & \text{for IH,} \end{cases} \tag{63}$$

In 3σ range of s_{13} [1], $2.000 \times 10^{-2} < s_{13}^2 < 2.405 \times 10^{-2}$ for NH and $2.018 \times 10^{-2} < s_{13}^2 < 2.424 \times 10^{-2}$

for IH; thus, Eq. (40) implies that

$$s_{12}^2 \in \begin{cases} (0.3401, 0.3415) & \text{for NH,} \\ (0.3402, 0.3416) & \text{for IH,} \end{cases} \quad (64)$$

i.e.,

$$\theta_{12}(\circ) \in \begin{cases} (35.68, 35.76) & \text{for NH,} \\ (35.68, 35.77) & \text{for IH,} \end{cases} \quad (65)$$

which all belong to 3σ range of s_{12}^2 [1] as given in Tab. I.

Next, using the constraints of k_0 in Eq. (63) and the 3σ range of reactor mixing angle s_{13} , i.e., $s_{13}^2 \in (2.00, 2.405)10^{-2}$ for NH and $s_{13}^2 \in (2.018, 2.424)10^{-2}$ for IH, from Eq. (46), we can depict the dependence of k_3^2 on k_0^2 and s_{13}^2 as shown in Fig. 2, which implies that

$$k_3^2 \in \begin{cases} (0.17, 0.22) & \text{for NH,} \\ (0.948, 0.956) & \text{for IH.} \end{cases} \quad (66)$$

Equation (41) shows that s_{23}^2 depends on k_0, k_3 and $\sin \alpha_1$. At the best-fit values of Δm_{21}^2 and

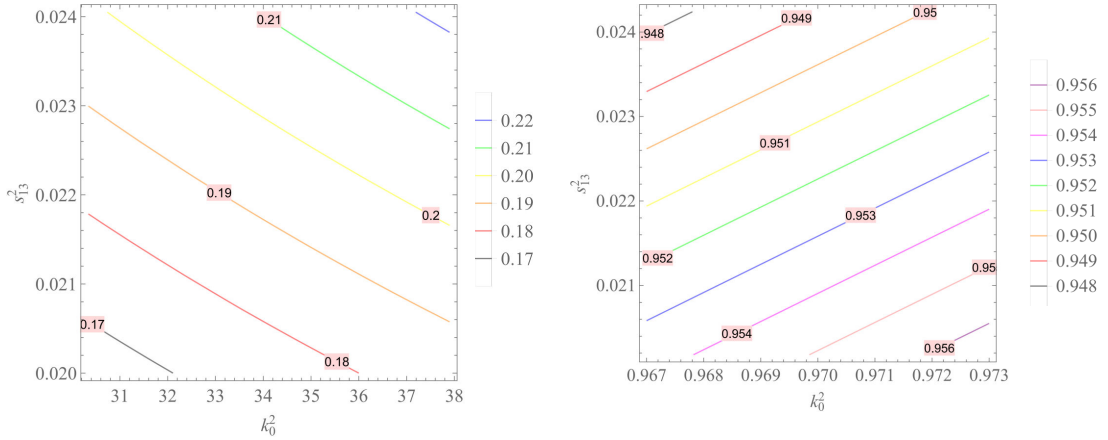


Figure 2. The contour plot of k_3^2 as a function of k_0^2 and s_{13}^2 with $k_0^2 \in (30.34, 37.9)$ and $s_{13}^2 \in (2.00, 2.405)10^{-2}$ for NH (left panel) while $k_0^2 \in (0.967, 0.973)$ and $s_{13}^2 \in (2.018, 2.424)10^{-2}$ for IH (right panel).

Δm_{31}^2 , we get

$$m_0^2 = \begin{cases} 75.0 \text{ meV}^2 & \text{for NH,} \\ 2525.0 \text{ meV}^2 & \text{for IH,} \end{cases} \quad k_0^2 = \begin{cases} 34.0 & \text{for NH,} \\ 0.9703 & \text{for IH,} \end{cases} \quad (67)$$

$$\begin{cases} m_1 = 0 \text{ meV}, m_2 = 8.66 \text{ meV}, m_3 = 50.50 \text{ meV} & \text{for NH,} \\ m_1 = 49.50 \text{ meV}, m_2 = 50.25 \text{ meV}, m_3 = 0 \text{ meV} & \text{for IH,} \end{cases} \quad (68)$$

and we find the ranges of $\sin \alpha_1$ that of s_{23}^2 lies in 3σ range given in Table I as depicted in Fig. 3 which implies

$$s_{23}^2 \in \begin{cases} (0.46, 0.54) & \text{for NH,} \\ (0.44, 0.60) & \text{for IH.} \end{cases} \quad (69)$$

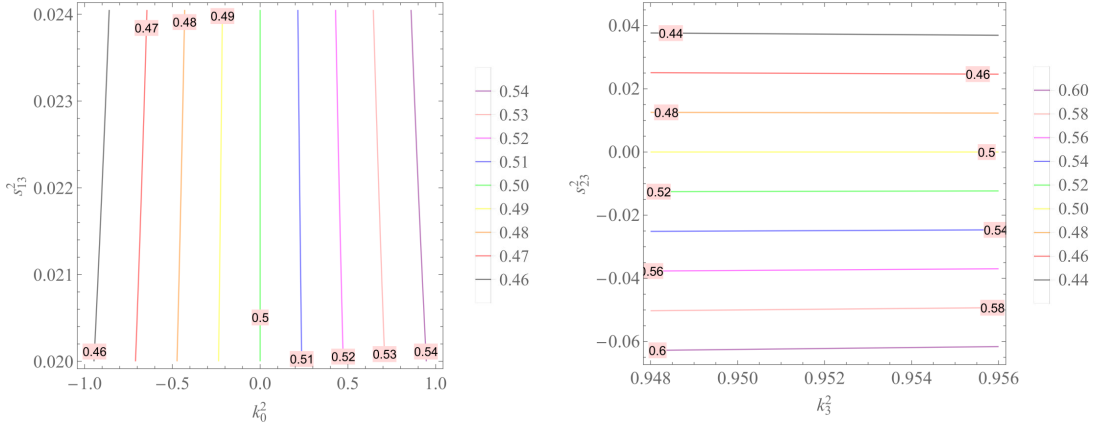


Figure 3. s_{23}^2 versus k_0^2 and $\sin \alpha_1$ with $k_0^2 \in (0.17, 0.22)$ and $\sin \alpha_1 \in (-1, 1)$ for NH (left panel) while $k_0^2 \in (0.948, 0.956)$ and $\sin \alpha_1 \in (-0.065, 0.045)$ for IH (right panel).

Further, Eqs. (42) and (45)-(47) imply that, at the best-fit values of Δm_{21}^2 and Δm_{31}^2 , k_2 and $\sin \delta_{CP}$ depend on two parameters θ_{13} and θ_{23} which are plotted in Figs. 4 and 5, respectively. These figures indicates that

$$k_2 \in \begin{cases} (2.00, 3.40) & \text{for NH,} \\ (0.68, 0.80) & \text{for IH,} \end{cases} \quad (70)$$

$$\sin \delta_{CP} \in \begin{cases} (-0.60, -0.20) & \text{for NH,} \\ (-0.95, -0.60) & \text{for IH,} \end{cases} \quad (71)$$

At present, there are various experimental bounds on Δm_{41}^2 [2, 4–8, 10–15, 19], for example, $\Delta m_{41}^2 \in (0.01, 1.0) \text{ eV}^2$ [4], $\Delta m_{41}^2 > 10^{-2} \text{ eV}^2$ [11], $\Delta m_{41}^2 = 0.041 \text{ eV}^2$ [10], $\Delta m_{41}^2 \in (0.1, 1.0) \text{ eV}^2$ [6], $\Delta m_{41}^2 \in (0.2, 10.0) \text{ eV}^2$ [2], $\Delta m_{41}^2 \geq 0.1 \text{ eV}^2$ [5], $\Delta m_{41}^2 = 1.0 \text{ eV}^2$ [14, 15], $\Delta m_{41}^2 > 1.5 \text{ eV}^2$ [7], $\Delta m_{41}^2 = 1.7 \text{ eV}^2$ [19], $\Delta m_{41}^2 < 10.0 \text{ eV}^2$ [12], $\Delta m_{41}^2 = 1.45 \text{ eV}^2$ [13]. Expressions (40)-(46), (48), (53)-(55) implies that $|U_{14}|^2$, $|U_{24}|^2$ and $|U_{34}|^2$ depend on five experimental parameters Δm_{21}^2 , Δm_{31}^2 , Δm_{41}^2 , $\sin^2 \theta_{13}$ and $\sin^2 \theta_{23}$. At the best-fit values of Δm_{21}^2 , Δm_{31}^2 and s_{13}^2 , three mixing elements $|U_{14}|^2$, $|U_{24}|^2$ and $|U_{34}|^2$ depend on two parameters m_s (or Δm_{41}^2) and θ_{23} . We found

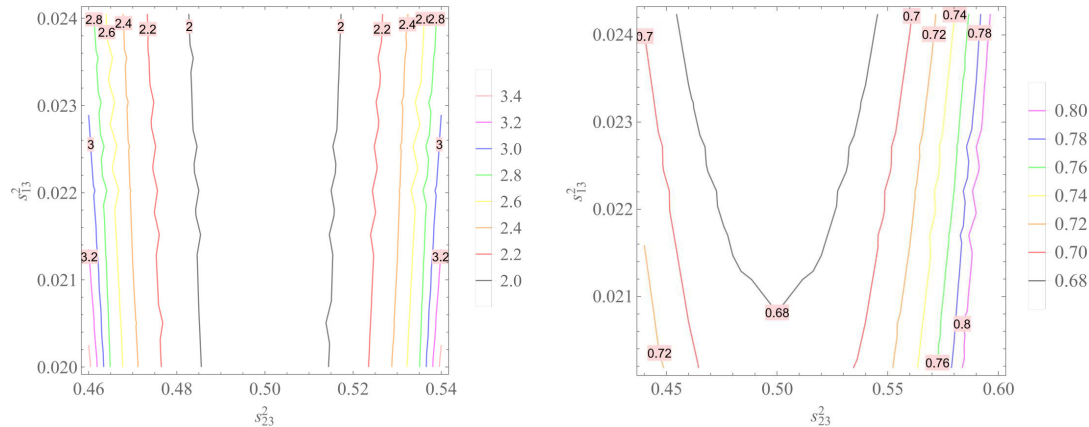


Figure 4. k_2 versus s_{13}^2 and s_{23}^2 with $s_{13}^2 \in (2.00, 2.405) 10^{-2}$ and $s_{23}^2 \in (0.46, 0.54)$ for NH (left panel) while $s_{13}^2 \in (2.018, 2.424) 10^{-2}$ and $s_{23}^2 \in (0.44, 0.60)$ for IH (right panel).

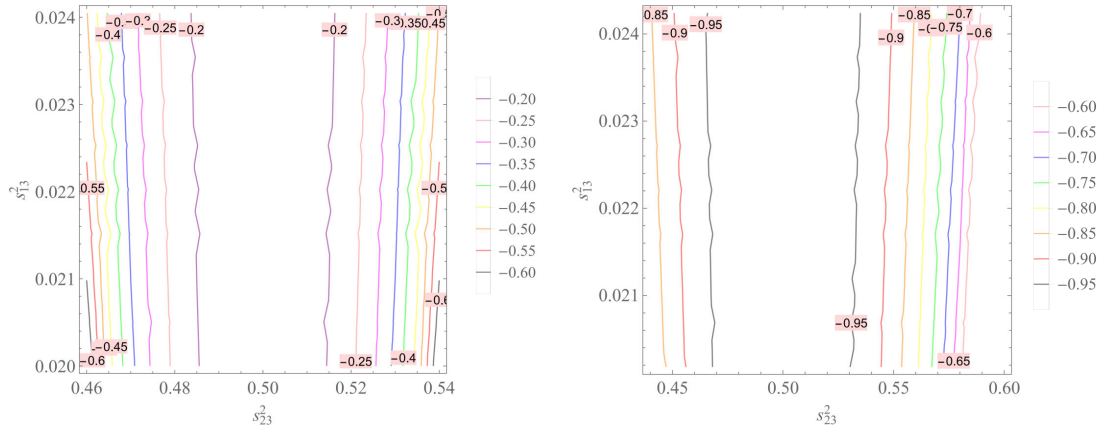


Figure 5. $\sin \delta_{CP}$ versus s^2_{13} and s^2_{23} with $s^2_{13} \in (2.00, 2.405) 10^{-2}$ and $s^2_{23} \in (0.46, 0.54)$ for NH (left panel) while $s^2_{13} \in (2.018, 2.424) 10^{-2}$ and $s^2_{23} \in (0.44, 0.60)$ for IH (right panel).

the possible values of Δm_{41}^2 and θ_{23} with $\Delta m_{41}^2 \in (0.5, 10.0) \text{ eV}^2$, $s_{23}^2 \in (0.46, 0.54)$ for NH and $\Delta m_{41}^2 \in (7.0, 50.0) \text{ eV}^2$, $s_{23}^2 \in (0.44, 0.60)$ for IH that satisfy the experimental constraints on $|U_{14}|^2$, $|U_{24}|^2$ and $|U_{34}|^2$ are shown in Table I which are plotted in Figs. 6, 7 and 8. Thus in this work, Δm_{41}^2 is chosen in the range of $\Delta m_{41}^2 \in (0.5, 10) \text{ eV}^2$ for NH while $\Delta m_{41}^2 \in (7.0, 50.0) \text{ eV}^2$ for IH, and Eq. (49) implies

$$m_s \in \begin{cases} (707.11, 3162.28) \text{ meV} & \text{for NH,} \\ (2646.22, 7071.24) \text{ meV} & \text{for IH.} \end{cases} \quad (72)$$

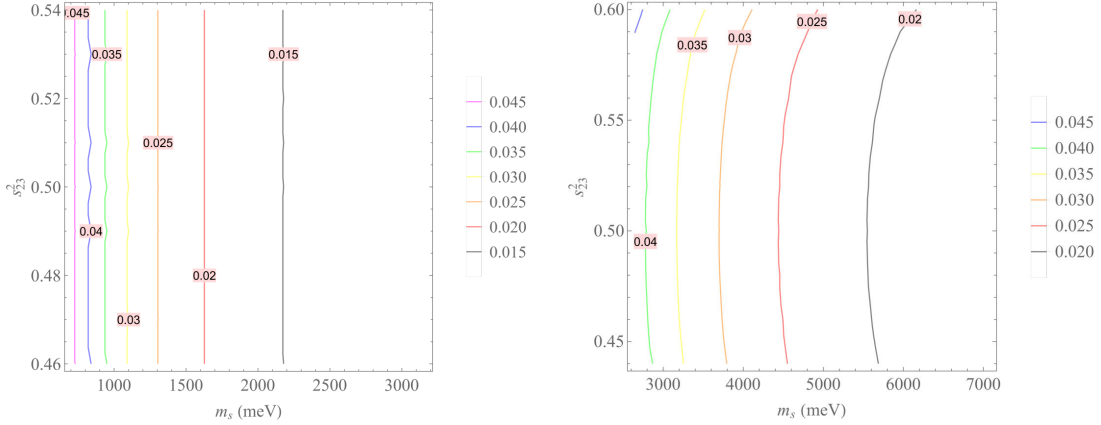


Figure 6. The contour plot of $|U_{14}|^2$ as a function of m_s and s_{23}^2 with $m_s \in (707.11, 3162.28)$ meV [i.e., $\Delta m_{41}^2 \in (0.5, 10.0)$ eV 2] and $s_{23}^2 \in (0.46, 0.54)$ for NH (left panel) while $m_s \in (2646.22, 7071.24)$ meV [i.e., $\Delta m_{41}^2 \in (7.0, 50.0)$ eV 2] and $s_{23}^2 \in (0.44, 0.60)$ for IH (right panel).

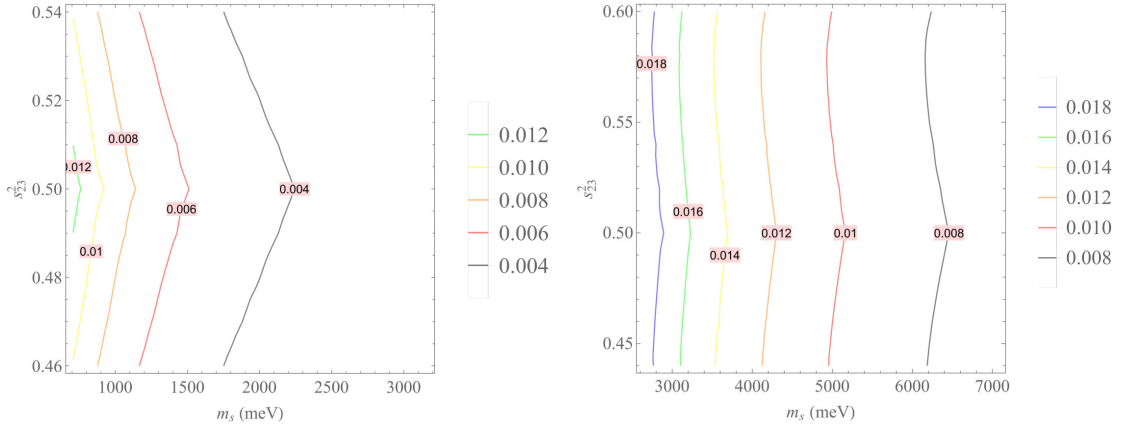


Figure 7. The contour plot of $|U_{24}|^2$ as a function of m_s and s_{23}^2 with $m_s \in (707.11, 3162.28)$ meV [i.e., $\Delta m_{41}^2 \in (0.5, 10.0)$ eV 2] and $s_{23}^2 \in (0.46, 0.54)$ for NH (left panel) while $m_s \in (2646.22, 7071.24)$ meV [i.e., $\Delta m_{41}^2 \in (7.0, 50.0)$ eV 2] and $s_{23}^2 \in (0.44, 0.60)$ for IH (right panel).

Figures 6, 7 and 8 show that our model predicts the range of $|U_{e4}|^2$, $|U_{\mu 4}|^2$ and $|U_{\tau 4}|^2$ as follows

$$|U_{14}|^2 \in \begin{cases} (0.015, 0.045) & \text{for NH,} \\ (0.020, 0.045) & \text{for IH,} \end{cases} \quad (73)$$

$$|U_{24}|^2 \in \begin{cases} (0.004, 0.012) & \text{for NH,} \\ (0.008, 0.018) & \text{for IH,} \end{cases} \quad (74)$$

$$|U_{34}|^2 \in \begin{cases} (0.004, 0.014) & \text{for NH,} \\ (0.008, 0.022) & \text{for IH.} \end{cases} \quad (75)$$

Further, Eqs. (43)–(46) and (53)–(57) imply that $\langle m_{ee} \rangle$, $\langle m_{ee}^{(3)} \rangle$ and $m_{\beta}^{(3)}$ depend on four parameters Δm_{21}^2 , Δm_{31}^2 , θ_{13} and θ_{23} while m_{β} , $|U_{e4}|^2$, $|U_{\mu 4}|^2$ and $|U_{\tau 4}|^2$ depend on five parameters

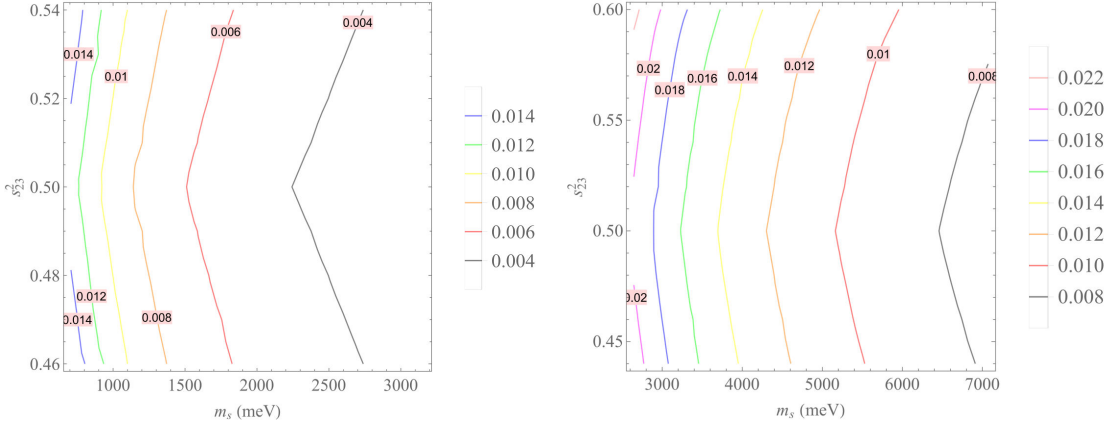


Figure 8. The contour plot of $|U_{34}|^2$ as a function of m_s and s_{23}^2 with $m_s \in (707.11, 3162.28)$ meV [i.e., $\Delta m_{41}^2 \in (0.5, 10.0)$ eV 2] and $s_{23}^2 \in (0.46, 0.54)$ for NH (left panel) while $m_s \in (2646.22, 7071.24)$ meV [i.e., $\Delta m_{41}^2 \in (7.0, 50.0)$ eV 2] and $s_{23}^2 \in (0.44, 0.60)$ for IH (right panel).

$\Delta m_{21}^2, \Delta m_{31}^2, \theta_{13}, \theta_{23}$ and m_s . At the best-fit values of $\Delta m_{21}^2, \Delta m_{31}^2$ taken from Table I, we get

$$k_3^2 = \begin{cases} 0.1924 & \text{for NH,} \\ 0.9522 & \text{for IH,} \end{cases} \quad (76)$$

and the effective neutrino masses $\langle m_{ee} \rangle$, $\langle m_{e\bar{e}}^{(3)} \rangle$ and $m_\beta^{(3)}$ depend on θ_{13} and θ_{23} which is depicted in Figs. 9, 10 and 11.

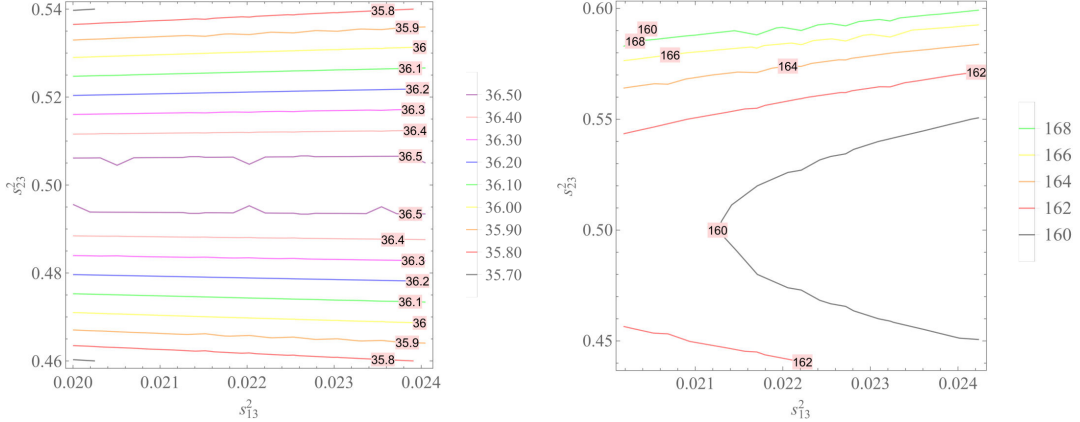


Figure 9. $\langle m_{ee} \rangle$ versus s_{13}^2 and s_{23}^2 with $s_{13}^2 \in (2.00, 2.405)10^{-2}$ and $s_{23}^2 \in (0.46, 0.54)$ for NH (left panel) while $s_{13}^2 \in (2.018, 2.424)10^{-2}$ and $s_{23}^2 \in (0.44, 0.60)$ for IH (right panel).

At the best-fit values of $\Delta m_{21}^2, \Delta m_{31}^2$ and $s_{13}^2, m_\beta, |U_{e4}|^2, |U_{\mu 4}|^2$ and $|U_{\tau 4}|^2$ depend on m_s and θ_{23} which are plotted in Figs. 12, 6, 7 and 8. Figures 9–12 show that our model predicts the range

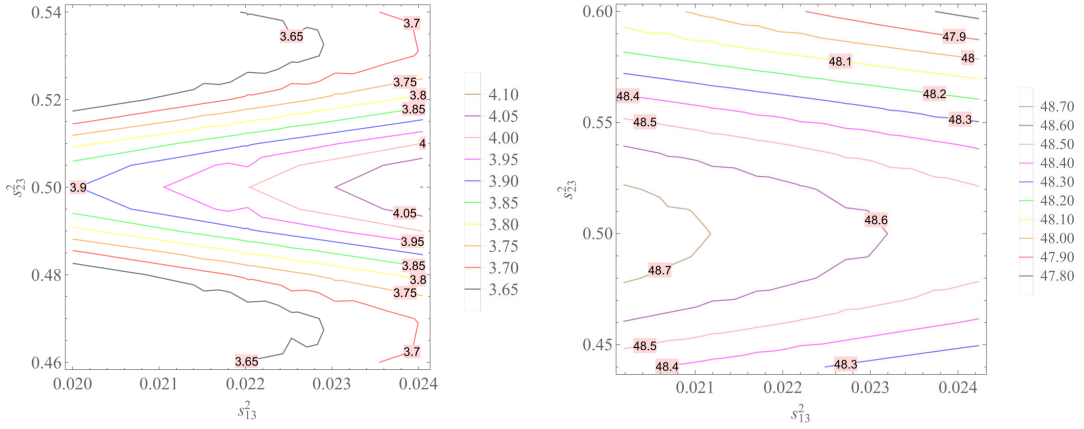


Figure 10. $\langle m_{ee}^{(3)} \rangle$ versus s_{13}^2 and s_{23}^2 with $s_{13}^2 \in (2.00, 2.405)10^{-2}$ and $s_{23}^2 \in (0.46, 0.54)$ for NH (left panel) while $s_{13}^2 \in (2.018, 2.424)10^{-2}$ and $s_{23}^2 \in (0.44, 0.60)$ for IH (right panel).

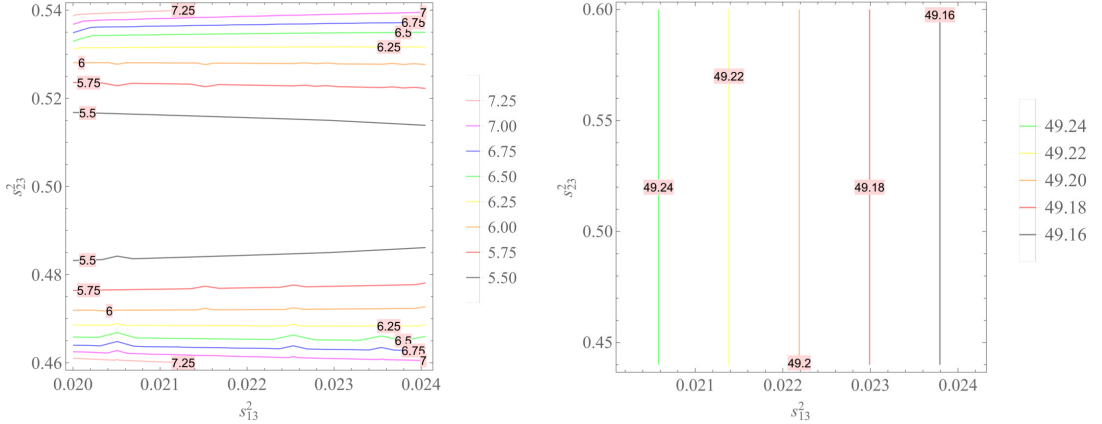


Figure 11. The contour plot of $m_\beta^{(3)}$ as a function of s_{13}^2 and s_{23}^2 with $s_{13}^2 \in (2.00, 2.405)10^{-2}$ and $s_{23}^2 \in (0.46, 0.54)$ for NH (left panel) while $s_{13}^2 \in (2.018, 2.424)10^{-2}$ and $s_{23}^2 \in (0.44, 0.60)$ for IH (right panel).

of the effective neutrino mass parameters as follows

$$\langle m_{ee} \rangle \in \begin{cases} (35.70, 36.50) \text{ meV for NH}, \\ (160.0, 168.0) \text{ meV for IH}, \end{cases} \quad (77)$$

$$\langle m_{ee}^{(3)} \rangle \in \begin{cases} (3.65, 4.10) \text{ meV for NH}, \\ (47.80, 48.70) \text{ meV for IH}, \end{cases} \quad (78)$$

$$m_\beta^{(3)} \in \begin{cases} (5.50, 7.25) \text{ meV for NH}, \\ (49.16, 49.24) \text{ meV for IH}, \end{cases} \quad (79)$$

$$m_\beta \in \begin{cases} (160.0, 320.0) \text{ meV for NH}, \\ (550.0, 900.0) \text{ meV for IH}. \end{cases} \quad (80)$$

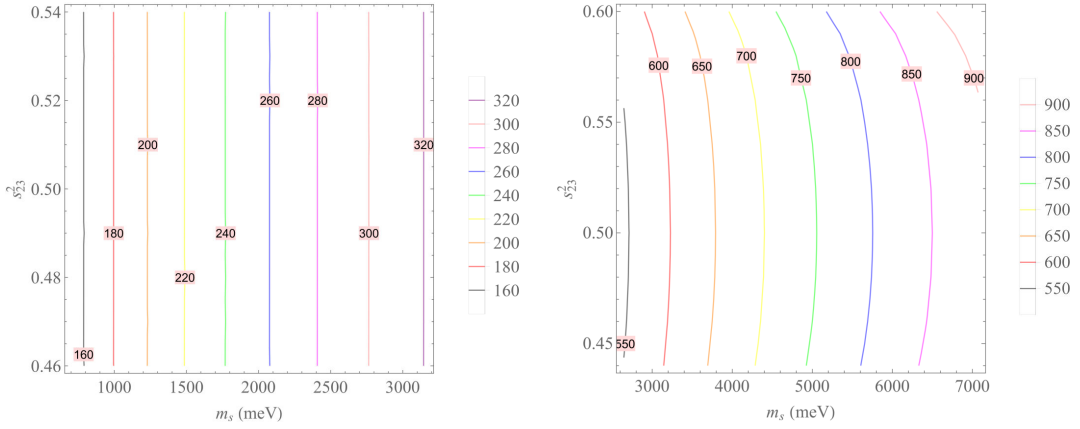


Figure 12. The contour plot of m_β as a function of m_s and s_{23}^2 with $m_s \in (707.11, 3162.28)$ meV [i.e., $\Delta m_{41}^2 \in (0.5, 10.0)$ eV 2] and $s_{23}^2 \in (0.46, 0.54)$ for NH (left panel) while $m_s \in (2646.22, 7071.24)$ meV [i.e., $\Delta m_{41}^2 \in (7.0, 50.0)$ eV 2] and $s_{23}^2 \in (0.44, 0.60)$ for IH (right panel).

We see that the resulting effective neutrino mass for three neutrino scheme in Eq. (78), for both normal and inverted hierarchies, are below all the upper bounds taken from GERDA [119] $\langle m_{ee} \rangle < 120 \div 260$ meV, MAJORANA [120] $\langle m_{ee} \rangle < 24 \div 53$ meV, CUORE [121] $\langle m_{ee} \rangle < 110 \div 500$ meV, KamLAND-Zen [122] $\langle m_{ee} \rangle < 61 \div 165$ meV, GERDA [123] $\langle m_{ee} \rangle < 104 \div 228$ meV and CUORE [124] $\langle m_{ee} \rangle < 75 \div 350$ meV. Furthermore, the resulting effective neutrino mass for 3+1 scheme in Eq. (77) are below all the upper bounds taken from CUPID-Mo experiment [125], $\langle m_{ee} \rangle < 300 \div 500$ meV.

Finally, from the above analysis, we can summarize the obtained parameters of the model as shown in Table III.

Table III. The model prediction compared to the experimental range

Parameters	Prediction (NH)	Experimental range (NH)	Prediction (IH)	Experimental range (IH)
$\sin^2 \theta_{12}$	$0.3401 \rightarrow 0.3415$	$0.271 \rightarrow 0.369$	$0.3402 \rightarrow 0.3416$	$0.271 \rightarrow 0.369$
$\sin^2 \theta_{23}$	$0.460 \rightarrow 0.540$	$0.434 \rightarrow 0.610$	$0.44 \rightarrow 0.60$	$0.433 \rightarrow 0.608$
$\delta_{CP}(\circ)$	$-0.60 \rightarrow -0.20$	$-1.0 \rightarrow 0.79$	$-0.95 \rightarrow -0.6$	$-1.0 \rightarrow -0.125$
$ U_{14} ^2$	$0.015 \rightarrow 0.045$	$0.012 \rightarrow 0.047$	$0.020 \rightarrow 0.045$	$0.012 \rightarrow 0.047$
$ U_{24} ^2$	$0.004 \rightarrow 0.012$	$0.005 \rightarrow 0.03$	$0.008 \rightarrow 0.018$	$0.005 \rightarrow 0.03$
$ U_{34} ^2$	$0.004 \rightarrow 0.014$	$0 \rightarrow 0.16$	$0.008 \rightarrow 0.022$	$0 \rightarrow 0.16$

In the case $s_{23}^2 = 0.47$ ($\theta_{23} = 43.30^\circ$) and $\Delta m_{41}^2 = 1.45$ eV 2 [13] for NH while $s_{23}^2 = 0.578$ ($\theta_{23} = 49.50^\circ$) and $\Delta m_{41}^2 = 15.0$ eV 2 ($m_s = 1873.30$ meV) for IH, we get the explicit parameters as listed

in Tab. IV.

Table IV. The obtained parameters

Parameters	The derived values (NH)	The derived values (IH)
k_2	1.54	0.868
$\alpha_1(\circ)$	137.50	352.34
$\delta_{CP}(\circ)$	160.20	316.70
m_s (eV)	1.204	3.873
$ U_{14} ^2$	0.027	0.0301
$ U_{24} ^2$	0.00622	0.0127
$ U_{34} ^2$	0.00883	0.0147
$\langle m_{ee} \rangle$ (meV)	36.00	164.00
$\langle m_{ee}^{(3)} \rangle$ (meV)	3.61	48.10
m_β (meV)	198.00	673.00
$m_\beta^{(3)}$ (meV)	6.12	49.20

VI. CONCLUSIONS

The combination of $B - L$ model and discrete symmetry $A_4 \times Z_3 \times Z_4$ can successfully explain both the active and the sterile mixing observables in 3+1 scheme. In the model, the tiny neutrino mass the mass hierarchy are obtained by the type-I seesaw mechanism and the minimal extended seesaw and the charged lepton mass hierarchy is satisfied by a factor of $v_H \left(\frac{v_L}{\Lambda}\right)^2 \sim 10^{-4}$ GeV of the electron mass compared to the muon and the tau masses of the order of $\frac{v_H v_L}{\Lambda} \sim 10^{-1}$ GeV. The observables are given in terms of five model parameters, $k_{2,3}$, m_0 , m_s and α_1 . The experimental ranges of the reactor mixing angle (s_{13}^2) and the two mass-squared differences (Δm_{21}^2 , Δm_{31}^2) are chosen to obtain the allowed values of s_{12} and k_3 for both NH and IH. The possible range values of $\sin \alpha_1$ gives the predictive range of s_{23} . α_1 and s_{13} are used to predict k_2 and δ_{CP} . The model parameter m_s (corresponds to the sterile neutrino mass) is determined by the active-sterile mass-squared difference Δm_{41}^2 for NH and by Δm_{41}^2 , Δm_{31}^2 and Δm_{21}^2 [Eqs. (43), (44) and (49)] for IH. The experimental ranges of s_{13} and the extracted values of s_{23} are used to evaluate the effective neutrino masses governing the neutrinoless double-beta decay while the extracted values of m_s and s_{23} are used to evaluate the active-sterile mixing.

The 3 + 1 active-sterile neutrino mixings are predicted to be $0.015 \leq |U_{14}|^2 \leq 0.045$, $0.004 \leq |U_{24}|^2 \leq 0.012$, $0.004 \leq |U_{34}|^2 \leq 0.014$ for normal hierarchy and $0.020 \leq |U_{14}|^2 \leq 0.045$, $0.008 \leq$

$|U_{24}|^2 \leq 0.018$, $0.008 \leq |U_{34}|^2 \leq 0.022$ for inverted hierarchy. Sterile neutrino masses are predicted to be $0.7 \lesssim m_s$ (eV) $\lesssim 3.16$ for normal hierarchy and $2.6 \lesssim m_s$ (eV) $\lesssim 7.1$ for inverted hierarchy. For three neutrino scheme the model predicts $0.3401 \leq \sin^2 \theta_{12} \leq 0.3415$, $0.460 \leq \sin^2 \theta_{23} \leq 0.540$, $-0.60 \leq \sin \delta_{CP} \leq -0.20$ for normal hierarchy and $0.3402 \leq \sin^2 \theta_{12} \leq 0.3416$, $0.434 \leq \sin^2 \theta_{23} \leq 0.610$, $-0.95 \leq \sin \delta_{CP} \leq -0.60$ for inverted hierarchy. The effective neutrino masses are predicted to be $35.70 \leq \langle m_{ee} \rangle$ [meV] ≤ 36.50 in 3+1 scheme and $3.65 \leq \langle m_{ee}^{(3)} \rangle$ [meV] ≤ 4.10 in three neutrino scheme for NH while $160.0 \leq \langle m_{ee} \rangle$ [meV] ≤ 168.0 in 3+1 scheme and $47.80 \leq \langle m_{ee}^{(3)} \rangle$ [meV] ≤ 48.70 in three neutrino scheme for IH which are all in agreement with the recent experimental bounds.

Appendix A: Higgs potential invariant under Γ symmetry

The total scalar potential invariant under Γ symmetry, up to five-dimension, is given by¹¹:

$$\begin{aligned} V_{\text{scalar}} = & V(H) + V(\phi_l) + V(\phi_\nu) + V(\eta) + V(\phi_s) \\ & + V(H, \phi_l) + V(H, \phi_\nu) + V(H, \eta) + V(H, \phi_s) + V(\phi_l, \phi_\nu) \\ & + V(\phi_l, \eta) + V(\phi_l, \phi_s) + V(\phi_\nu, \eta) + V(\phi_\nu, \phi_s) + V(\eta, \phi_s) + V_{\text{triple}}, \end{aligned} \quad (\text{A1})$$

where

$$V(H) = \mu_H^2 (H^\dagger H)_{\underline{1}} + \lambda_H (H^\dagger H)_{\underline{1}} (H^\dagger H)_{\underline{1}}, \quad (\text{A2})$$

$$\begin{aligned} V(\phi_l) = & \mu_{\phi_l}^2 (\phi_l^\dagger \phi_l)_{\underline{1}} + \lambda_1^{\phi_l} (\phi_l^\dagger \phi_l)_{\underline{1}} (\phi_l^\dagger \phi_l)_{\underline{1}} + \lambda_2^{\phi_l} (\phi_l^\dagger \phi_l)_{\underline{1}'} (\phi_l^\dagger \phi_l)_{\underline{1}''} \\ & + \lambda_3^{\phi_l} (\phi_l^\dagger \phi_l)_{\underline{1}''} (\phi_l^\dagger \phi_l)_{\underline{1}'} + \lambda_4^{\phi_l} (\phi_l^\dagger \phi_l)_{\underline{3}_s} (\phi_l^\dagger \phi_l)_{\underline{3}_s} + \lambda_5^{\phi_l} (\phi_l^\dagger \phi_l)_{\underline{3}_a} (\phi_l^\dagger \phi_l)_{\underline{3}_a}, \end{aligned} \quad (\text{A3})$$

$$V(\phi_\nu) = V(\phi_l \rightarrow \phi_\nu), \quad V(\eta) = V(H \rightarrow \eta), \quad V(\phi_s) = V(\phi_l \rightarrow \phi_s), \quad V(\eta_s) = V(\eta_s \rightarrow \eta), \quad (\text{A4})$$

$$V(H, \phi_l) = \lambda_1^{H\phi_l} (H^\dagger H)_{\underline{1}} (\phi_l^\dagger \phi_l)_{\underline{1}} + \lambda_2^{H\phi_l} (H^\dagger \phi_l)_{\underline{3}} (\phi_l^\dagger H)_{\underline{3}}, \quad V(H, \phi_\nu) = V(H, \phi_l \rightarrow \phi_\nu), \quad (\text{A5})$$

$$V(H, \eta) = \lambda_1^{H\eta} (H^\dagger H)_{\underline{1}} (\eta^\dagger \eta)_{\underline{1}} + \lambda_2^{H\eta} (H^\dagger \eta)_{\underline{1}} (\eta^\dagger H)_{\underline{1}}, \quad V(H, \phi_s) = V(H, \phi_l \rightarrow \phi_s), \quad (\text{A6})$$

$$\begin{aligned} V(H, \eta_s) = & V(H, \eta \rightarrow \eta_s), \quad V(\phi_l, \phi_\nu) = \lambda_1^{\phi_l \phi_\nu} (\phi_l^\dagger \phi_l)_{\underline{1}} (\phi_\nu^\dagger \phi_\nu)_{\underline{1}} + \lambda_2^{\phi_l \phi_\nu} (\phi_l^\dagger \phi_l)_{\underline{1}'} (\phi_\nu^\dagger \phi_\nu)_{\underline{1}''} \\ & + \lambda_3^{\phi_l \phi_\nu} (\phi_l^\dagger \phi_l)_{\underline{1}''} (\phi_\nu^\dagger \phi_\nu)_{\underline{1}'} + \lambda_4^{\phi_l \phi_\nu} (\phi_l^\dagger \phi_l)_{\underline{3}_s} (\phi_\nu^\dagger \phi_\nu)_{\underline{3}_s} + \lambda_5^{\phi_l \phi_\nu} (\phi_l^\dagger \phi_l)_{\underline{3}_a} (\phi_\nu^\dagger \phi_\nu)_{\underline{3}_a} \\ & + \lambda_6^{\phi_l \phi_\nu} (\phi_l^\dagger \phi_\nu)_{\underline{1}} (\phi_\nu^\dagger \phi_l)_{\underline{1}} + \lambda_7^{\phi_l \phi_\nu} (\phi_l^\dagger \phi_\nu)_{\underline{1}'} (\phi_\nu^\dagger \phi_l)_{\underline{1}''} + \lambda_8^{\phi_l \phi_\nu} (\phi_l^\dagger \phi_\nu)_{\underline{1}''} (\phi_\nu^\dagger \phi_l)_{\underline{1}'} \\ & + \lambda_9^{\phi_l \phi_\nu} (\phi_l^\dagger \phi_\nu)_{\underline{3}_s} (\phi_\nu^\dagger \phi_l)_{\underline{3}_s} + \lambda_{10}^{\phi_l \phi_\nu} (\phi_l^\dagger \phi_\nu)_{\underline{3}_a} (\phi_\nu^\dagger \phi_l)_{\underline{3}_a}, \quad V(\phi_l, \eta) = V(\phi_l, H \rightarrow \eta), \end{aligned} \quad (\text{A7})$$

¹¹ Here, $V(\alpha_1 \rightarrow \alpha_2, \beta_1 \rightarrow \beta_2, \dots) \equiv V(\alpha_1, \beta_1, \dots)_{\{\alpha_1=\alpha_2, \beta_1=\beta_2, \dots\}}$.

$$V(\phi_l, \phi_s) = V(\phi_l, \phi_\nu \rightarrow \phi_s), \quad V(\phi_l, \eta_s) = V(\phi_l, \eta \rightarrow \eta_s), \quad V(\phi_\nu, \eta) = V(\phi_l \rightarrow \phi_\nu, \eta), \quad (\text{A8})$$

$$V(\phi_\nu, \phi_s) = V(\phi_l \rightarrow \phi_\nu, \phi_s), \quad V(\phi_\nu, \eta_s) = V(\phi_\nu, \eta \rightarrow \eta_s), \quad V(\phi_s, \eta) = V(\phi_l \rightarrow \phi_s, \eta), \quad (\text{A9})$$

$$V(\eta, \eta_s) = \lambda_1^{\eta\eta_s}(\eta^\dagger\eta)(\eta_s^\dagger\eta_s) + \lambda_1^{\eta\eta_s}(\eta_s^\dagger\eta)(\eta^\dagger\eta_s), \quad V(\phi_s, \eta_s) = V(\phi_s, \eta \rightarrow \eta_s), \quad (\text{A10})$$

$$\begin{aligned} V_{\text{triple}} = & \lambda_1^{H\phi_l\phi_s}(H^\dagger H)\underline{1}(\phi_l^\dagger\phi_l)\underline{3}_s\phi_\nu + \lambda_2^{H\phi_l\phi_s}(H^\dagger H)\underline{1}(\phi_l^\dagger\phi_l)\underline{3}_a\phi_\nu \\ & + \lambda_1^{H\phi_s\phi_\nu}(H^\dagger H)\underline{1}(\phi_s^\dagger\phi_s)\underline{3}_s\phi_\nu + \lambda_2^{H\phi_s\phi_\nu}(H^\dagger H)\underline{1}(\phi_s^\dagger\phi_s)\underline{3}_a\phi_\nu \\ & + \lambda_1^{\phi_l\phi_\nu\eta}(\eta^\dagger\eta)\underline{1}(\phi_l^\dagger\phi_l)\underline{3}_s\phi_\nu + \lambda_2^{\phi_l\phi_\nu\eta}(\eta^\dagger\eta)\underline{1}(\phi_l^\dagger\phi_l)\underline{3}_a\phi_\nu \\ & + \lambda_1^{\phi_l\phi_\nu\phi_s}(\phi_l^\dagger\phi_l)\underline{3}_s\phi_\nu(\phi_s^\dagger\phi_s)\underline{1} + \lambda_2^{\phi_l\phi_\nu\phi_s}(\phi_l^\dagger\phi_l)\underline{3}_a\phi_\nu(\phi_s^\dagger\phi_s)\underline{1} \\ & + \lambda_3^{\phi_l\phi_\nu\phi_s}(\phi_s^\dagger\phi_s)\underline{3}_s\phi_\nu(\phi_l^\dagger\phi_l)\underline{1} + \lambda_4^{\phi_l\phi_\nu\phi_s}(\phi_s^\dagger\phi_s)\underline{3}_a\phi_\nu(\phi_l^\dagger\phi_l)\underline{1} \\ & + \lambda_5^{\phi_l\phi_\nu\phi_s}(\phi_l^\dagger\phi_s)\underline{3}_s\phi_\nu(\phi_s^\dagger\phi_l)\underline{1} + \lambda_6^{\phi_l\phi_\nu\phi_s}(\phi_l^\dagger\phi_s)\underline{3}_a\phi_\nu(\phi_s^\dagger\phi_l)\underline{1} \\ & + \lambda_7^{\phi_l\phi_\nu\phi_s}(\phi_s^\dagger\phi_l)\underline{3}_s\phi_\nu(\phi_l^\dagger\phi_s)\underline{1} + \lambda_8^{\phi_l\phi_\nu\phi_s}(\phi_s^\dagger\phi_l)\underline{3}_a\phi_\nu(\phi_l^\dagger\phi_s)\underline{1} \\ & + \lambda_1^{\phi_\nu\eta\phi_s}(\eta^\dagger\eta)\underline{1}(\phi_s^\dagger\phi_s)\underline{3}_s\phi_\nu + \lambda_2^{\phi_\nu\eta\phi_s}(\eta^\dagger\eta)\underline{1}(\phi_s^\dagger\phi_s)\underline{3}_a\phi_\nu \\ & + \lambda^{\phi_l\phi_\nu\eta_s}(\phi_l^*\phi_l)\underline{3}_s\phi_\nu(\eta_s^*\eta_s)\underline{1} + \lambda^{\phi_\nu\phi_s\eta_s}(\phi_s^*\phi_s)\underline{3}_s\phi_\nu(\eta_s^*\eta_s)\underline{1}. \end{aligned} \quad (\text{A11})$$

All the other triple, quartic and quintic terms, up to five-dimension, of three or four or five differential scalar fields are forbidden by one (or some) of the model symmetries, for instance, $(H^\dagger H)\underline{1}(\phi_l^\dagger\phi_\nu)\underline{1}$, $(H^\dagger H)\underline{1}(\phi_\nu^\dagger\phi_\nu)\underline{3}_s\phi_l$ and $(H^\dagger H)\underline{1}(\phi_\nu^\dagger\phi_\nu)\underline{3}_s\phi_l$ are forbidden by Z_3 and Z_4 ; $(H^\dagger H)\underline{1}(\eta^\dagger\eta)\underline{1}\phi_l$ is forbidden by A_4 , Z_3 and Z_4 ; $(H^\dagger H)\underline{1}\phi_l\phi_\nu\eta$ is forbidden by $U(1)_{B-L}$ and so on.

Appendix B: The solution of Eqs. (8)–(12)

$$\lambda^H = -\frac{\mu_H^2 + 3\lambda^{H\phi_l}v_l^2 + \lambda^{H\phi_\nu}v_\nu^2 + \lambda^{H\eta}v_\eta^2 + 2\lambda^{H\phi_s}v_s^2 + 2\Lambda^{H\phi_l\phi_\nu\phi_s}v_\nu + \lambda^{H\eta_s}v_{\eta_s}^2}{2v_H^2}, \quad (\text{B1})$$

$$\begin{aligned} \lambda^{\phi_l} &= -\frac{3\mu_{\phi_l}^2 + 3\lambda^{H\phi_l}v_H^2 + \lambda^{\phi_l\phi_\nu}v_\nu^2 + \lambda^{\phi_l\phi_s}v_s^2 + 3\lambda^{\phi_l\eta}v_\eta^2 + 2\Lambda_1^{H\phi_l\phi_\nu\phi_s\eta}v_\nu}{6v_l^2} \\ &\quad - \frac{(3\lambda^{\phi_l\eta_s} + 2\lambda^{\phi_l\phi_\nu\eta_s}v_\nu)v_{\eta_s}^2}{6v_l^2}, \end{aligned} \quad (\text{B2})$$

$$\begin{aligned} \lambda^{\phi_\nu} &= -\frac{\mu_\nu^2 + \lambda^{H\phi_\nu}v_H^2 + \lambda^{\phi_l\phi_\nu}v_l^2 + \lambda^{\phi_\nu\eta}v_\eta^2 - \lambda^{\phi_\nu\phi_s}v_s^2}{2v_\nu^2} - \frac{\Lambda_2^{H\phi_l\phi_\nu\eta\phi_s}v_l^2 + \Lambda_3^{H\phi_l\phi_\nu\eta\phi_s}v_s^2}{2v_\nu^3} \\ &\quad - \frac{(\Lambda^{\phi_l\phi_\nu\eta_s}v_l^2 + \Lambda^{\phi_\nu\phi_s\eta_s}v_s^2 + \Lambda^{\phi_\nu\eta_s}v_\nu)v_{\eta_s}^2}{2v_\nu^3}, \end{aligned} \quad (\text{B3})$$

$$\begin{aligned} \lambda^\eta &= -\frac{\mu_\eta^2 + \lambda^{H\eta}v_H^2 + 3\lambda^{\phi_l\eta}v_l^2 + \lambda^{\phi_\nu\eta}v_\nu^2 + 2\lambda^{\phi_s\eta}v_s^2 + 2(\lambda_1^{\phi_l\phi_\nu\eta}v_l^2 + \lambda^{\phi_\nu\eta\phi_s}v_s^2)v_\nu + \lambda^{\eta_s}v_{\eta_s}^2}{2v_\eta^2}, \quad (\text{B4}) \\ &\quad (B5) \end{aligned}$$

$$\begin{aligned} \lambda^{\phi_s} &= -\frac{2\mu_s^2 + 2\lambda^{H\phi_s}v_H^2 + \lambda^{\phi_l\phi_s}v_l^2 - \lambda^{\phi_\nu\phi_s}v_\nu^2 + 2\lambda^{\phi_s\eta}v_\eta^2 + 2\Lambda_3^{H\phi_l\phi_\nu\eta\phi_s}v_\nu}{2v_s^2} \\ &\quad - \frac{(\lambda^{\phi_s\eta_s} + \lambda^{\phi_\nu\phi_s\eta_s}v_\nu)v_{\eta_s}^2}{v_s^2}, \end{aligned} \quad (\text{B6})$$

$$\begin{aligned} \lambda^{\eta_s} &= -\frac{\mu_{\eta_s}^2 + \lambda^{\eta_s}v_\eta^2 + \lambda^{H\eta_s}v_H^2 + 2\lambda^{\phi_l\phi_\nu\eta_s}v_l^2v_\nu + 3\lambda^{\phi_l\eta_s}v_l^2 + \lambda^{\phi_\nu\eta_s}v_\nu^2}{2v_{\eta_s}^2} \\ &\quad - \frac{(\lambda^{\phi_\nu\phi_s\eta_s}v_\nu + \lambda^{\phi_s\eta_s})v_s^2}{v_{\eta_s}^2}. \end{aligned} \quad (\text{B7})$$

- [1] P. F. de Salas *et. al.*, *2020 Global reassessment of the neutrino oscillation picture*, J. High Energ. Phys. 2021, 71 (2021). [https://doi.org/10.1007/JHEP02\(2021\)071](https://doi.org/10.1007/JHEP02(2021)071).
- [2] A. Aguilar *et. al.* [LSND Collaboration], *Evidence for neutrino oscillations from the observation of $\bar{\nu}_e$ appearance in a $\bar{\nu}_\mu$ beam*, Phys. Rev. D 64 (2001) 112007. <https://doi.org/10.1103/PhysRevD.64.112007>.
- [3] M. Maltoni, T. Schwetz, M. Tortola and J. Valle, *Constraining neutrino oscillation parameters with current solar and atmospheric data*, Phys. Rev. D 67 (2003) 013011. <https://doi.org/10.1103/PhysRevD.67.013011>.
- [4] A. A. Aguilar-Arevalo *et. al.* [MiniBooNE Collaboration], *Improved Search for $\bar{\nu}_\mu \rightarrow \bar{\nu}_e$ Oscillations in the MiniBooNE Experiment*, Phys. Rev. Lett. 110 (2013) 161801. <https://doi.org/10.1103/PhysRevLett.110.161801>.

- [5] M. A. Acero, C. Giunti, M. Laveder, *Limits on $\nu_e \rightarrow \bar{\nu}_e$ disappearance from Gallium and reactor experiments*, Phys. Rev. D 78 (2008) 073009. <https://doi.org/10.1103/PhysRevD.78.073009>.
- [6] A. A. Aguilar-Arevalo *et al.* [MiniBooNE Collaboration], *Event excess in the MiniBooNE search for $\bar{\nu}_\mu \rightarrow \bar{\nu}_e$ oscillations*, Phys. Rev. Lett. 105 (2010) 181801. <https://doi.org/10.1103/PhysRevLett.105.181801>.
- [7] G. Mention *et al.*, *The Reactor Antineutrino Anomaly*, Phys. Rev. D 83 (2011) 073006. <https://doi.org/10.1103/PhysRevD.83.073006>.
- [8] F. P. An *et al.* [Daya Bay Collaboration], *Search for a Light Sterile Neutrino at Daya Bay*, Phys. Rev. Lett. 113 (2014) 141802. <https://doi.org/10.1103/PhysRevLett.113.141802>.
- [9] S. Gariazzo *et al.*, *Light sterile neutrinos*, J. Phys. G 43 (2016) 033001. <https://doi.org/10.1088/0954-3899/43/3/033001>.
- [10] A. A. Aguilar-Arevalo *et al.* [MiniBooNE Collaboration], *Significant Excess of ElectronLike Events in the MiniBooNE Short-Baseline Neutrino Experiment*, Phys. Rev. Lett. 121 (2018) 221801. <https://doi.org/10.1103/PhysRevLett.121.221801>.
- [11] P. Adamson *et al.* [MINOS+ Collaboration], *Search for sterile neutrinos in MINOS and MINOS+ using a two-detector fit*, Phys. Rev. Lett. 122 (2019) 091803. <https://doi.org/10.1103/PhysRevLett.122.091803>.
- [12] P. Adamson *et al.* [Daya Bay Collaboration, MINOS + Collaboration], *Improved Constraints on Sterile Neutrino Mixing from Disappearance Searches in the MINOS, MINOS+, Daya Bay, and Bugey-3 Experiments*, Phys. Rev. Lett. 125 (2020) 071801. <https://doi.org/10.1103/PhysRevLett.125.071801>.
- [13] M. G. Aartsen *et al.* [IceCube Collaboration], *An eV-scale sterile neutrino search using eight years of atmospheric muon neutrino data from the IceCube Neutrino Observatory*, Phys. Rev. Lett. 125 (2020) 141801. <https://doi.org/10.1103/PhysRevLett.125.141801>.
- [14] S. P. Behera, D. K. Mishrab, L. M. Pant, *Sensitivity to sterile neutrino mixing using reactor antineutrinos*, Eur. Phys. J. C 79 (2019) 86. <https://doi.org/10.1140/epjc/s10052-019-6591-0>.
- [15] S. P. Behera, D. K. Mishra, L. M. Pant, *Active-sterile neutrino mixing constraint using reactor antineutrinos with the ISMRAN set-up*, Phys. Rev. D 102 (2020) 013002. <https://doi.org/10.1103/PhysRevD.102.013002>.
- [16] S. K. Kang, Yeong-Duk Kim, Young-Ju Ko, K. Siyeon, *Four-neutrino analysis of 1.5km-baseline reactor antineutrino oscillations*, Adv. High Energy Phys. 2013 (2013) 138109. <https://doi.org/10.1155/2013/138109>.
- [17] Ivan Girardi *et. al.*, *Constraining Sterile Neutrinos Using Reactor Neutrino Experiments*, J. High Energ. Phys. 2014, 57 (2014). [https://doi.org/10.1007/JHEP08\(2014\)057](https://doi.org/10.1007/JHEP08(2014)057).
- [18] D. C. Rivera-Agudelo, A. Pérez-Lorenzana, *Generating θ_{13} from sterile neutrinos in $\mu - \tau$ symmetric models*, Phys. Rev. D 92 (2015) 073009. <https://doi.org/10.1103/PhysRevD.92.073009>.
- [19] S. Gariazzo, C. Giunti, M. Laveder, and Y. F. Li, *Updated Global 3+1 Analysis of Short-BaseLine Neutrino Oscillations*, J. High Energ. Phys. 2017, 135 (2017). [https://doi.org/10.1007/JHEP06\(2017\)135](https://doi.org/10.1007/JHEP06(2017)135).

- [20] Pilar Coloma, David V. Forero, Stephen J. Parke, *DUNE sensitivities to the mixing between sterile and tau neutrinos*, J. High Energ. Phys. 2018, 79 (2018). [https://doi.org/10.1007/JHEP07\(2018\)079](https://doi.org/10.1007/JHEP07(2018)079).
- [21] Jun-Hao Liu, Shun Zhou, *Another look at the impact of an eV-mass sterile neutrino on the effective neutrino mass of neutrinoless double-beta decays*, Int. J. Mod. Phys. A 33 (2018) 1850014. <https://doi.org/10.1142/S0217751X18500148>.
- [22] S. Gariazzo, C. Giunti, M. Laveder, Y.F. Li, *Model-Independent $\bar{\nu}_e$ Short-Baseline Oscillations from Reactor Spectral Ratios*, Phys. Lett. B 782 (2018) 13. <https://doi.org/10.1016/j.physletb.2018.04.057>.
- [23] Mona Dentler *et al.*, *Updated global analysis of neutrino oscillations in the presence of eV-scale sterile neutrinos*, J. High Energ. Phys. 2018, 10 (2018). [https://doi.org/10.1007/JHEP08\(2018\)010](https://doi.org/10.1007/JHEP08(2018)010).
- [24] Shivani Gupta, Zachary M. Matthews, Pankaj Sharma, Anthony G. Williams, *The Effect of a Light Sterile Neutrino at NO_νA and DUNE*, Phys. Rev. D 98 (2018) 035042. <https://doi.org/10.1103/PhysRevD.98.035042>.
- [25] Tarak Thakore, Moon Moon Devi, Sanjib Kumar Agarwalla, Amol Dighe, *Active-sterile neutrino oscillations at INO-ICAL over a wide mass-squared range*, J. High Energ. Phys. 2018, 22 (2018). [https://doi.org/10.1007/JHEP08\(2018\)022](https://doi.org/10.1007/JHEP08(2018)022).
- [26] S. Dev, DeshRaj, Radha Raman Gautam, Lal Singh, *New mixing schemes for (3+1) neutrinos*, Nucl. Phys. B 941 (2019) 401. <https://doi.org/10.1016/j.nuclphysb.2019.02.003>.
- [27] Luis Salvador Miranda, Soebur Razzaque, *Revisiting constraints on 3+1 active-sterile neutrino mixing using IceCube data*, J. High Energ. Phys. 2019, 203 (2019). [https://doi.org/10.1007/JHEP03\(2019\)203](https://doi.org/10.1007/JHEP03(2019)203).
- [28] C. Giunti, T. Lasserre, *eV-scale Sterile Neutrinos*, Annu. Rev. Nucl. Part. Sci. 69 (2019) 163. <https://doi.org/10.1146/annurev-nucl-101918-023755>.
- [29] Sebastian Böser *et al.*, *Status of Light Sterile Neutrino Searches*, Prog. Part. Nucl. Phys. 111 (2020) 103736. <https://doi.org/10.1016/j.ppnp.2019.103736>.
- [30] C. Giunti, Y.F. Li, Y.Y. Zhang, *KATRIN bound on 3+1 active-sterile neutrino mixing and the reactor antineutrino anomaly*, J. High Energ. Phys. 2020, 61 (2020). [https://doi.org/10.1007/JHEP05\(2020\)061](https://doi.org/10.1007/JHEP05(2020)061).
- [31] S. P. Behera, D. K. Mishra, L. M. Pant, *Active-sterile neutrino mixing constraint using reactor antineutrinos with the ISMRAN set-up*, Phys. Rev. D 102 (2020) 013002. <https://doi.org/10.1103/PhysRevD.102.013002>.
- [32] A. Diaz *et al.*, *Where Are We With Light Sterile Neutrinos?*, Phys. Rep. 884 (2020) 1. <https://doi.org/10.1016/j.physrep.2020.08.005>.
- [33] A. E. Nelson, *Effects of CP Violation from Neutral Heavy Fermions on Neutrino Oscillations, and the LSND/MiniBooNE Anomalies*, Phys. Rev. D84 (2011) 053001. <https://doi.org/10.1103/PhysRevD.84.053001>.
- [34] J. Fan and P. Langacker, *Light Sterile Neutrinos and Short Baseline Neutrino Oscillation Anomalies*, J. High Energ. Phys. 2012, 83 (2012). [https://doi.org/10.1007/JHEP04\(2012\)083](https://doi.org/10.1007/JHEP04(2012)083).

- [35] E. Kuflik, S. D. McDermott, and K. M. Zurek, *Neutrino Phenomenology in a 3+1+1 Framework*, Phys. Rev. D86 (2012) 033015. <https://doi.org/10.1103/PhysRevD.86.033015>.
- [36] J. Huang and A. E. Nelson, *MeV dark matter in the 3+1+1 model*, Phys. Rev. D88 (2013) 033016. <https://doi.org/10.1103/PhysRevD.88.033016>.
- [37] C. Giunti, M. Laveder, Y. Li, and H. Long, *A Pragmatic View of Short-Baseline Neutrino Oscillations*, Phys. Rev. D88 (2013) 073008. <https://doi.org/10.1103/PhysRevD.88.073008>.
- [38] J. Kopp, M. Maltoni, and T. Schwetz, *re there sterile neutrinos at the eV scale?*, Phys. Rev. Lett. 107 (2011) 091801. <https://doi.org/10.1103/PhysRevLett.107.091801>.
- [39] J. Kopp, P. A. N. Machado, M. Maltoni, and T. Schwetz, *Sterile Neutrino Oscillations: The Global Picture*, J. High Energ. Phys. 2013, 50 (2013). [https://doi.org/10.1007/JHEP05\(2013\)050](https://doi.org/10.1007/JHEP05(2013)050).
- [40] M. Sorel, J. Conrad, and M. Shaevitz, *A combined analysis of short-baseline neutrino experiments in the (3+1) and (3+2) sterile neutrino oscillation hypotheses*, Phys. Rev. D 70 (2004) 073004. <https://doi.org/10.1103/PhysRevD.70.073004>.
- [41] G. Karagiorgi *et al.*, *Leptonic CP violation studies at MiniBooNE in the (3+2) sterile neutrino oscillation hypothesis*, Phys. Rev. D75 (2007) 013011. <https://doi.org/10.1103/PhysRevD.75.013011>. [Erratum-*ibid.D* 80 (2009) 099902]
- [42] M. Maltoni and T. Schwetz, *Sterile neutrino oscillations after first MiniBooNE results*, Phys. Rev. D76 (2007) 093005. <https://doi.org/10.1088/1742-6596/110/8/082011>.
- [43] S. Goswami and W. Rodejohann, *MiniBooNE results and neutrino schemes with 2 sterile neutrinos: Possible mass orderings and observables related to neutrino masses*, JHEP10 (2007) 073. <https://doi.org/10.1088/1126-6708/2007/10/073>.
- [44] G. Karagiorgi *et al.*, *Viability of $\Delta m^2 \sim 1\text{eV}^2$ sterile neutrino mixing models in light of MiniBooNE electron neutrino and antineutrino data from the Booster and NuMI beamlines*, Phys. Rev. D80 (2009) 073001. <https://doi.org/10.1103/PhysRevD.80.073001>.
- [45] C. Giunti and M. Laveder, *3+1 and 3+2 Sterile Neutrino Fits*, Phys. Rev. D84 (2011) 073008. <https://doi.org/10.1103/PhysRevD.84.073008>.
- [46] A. Donini *et al.*, *The minimal 3+2 neutrino model versus oscillation anomalies*, J. High Energ. Phys. 2012, 161 (2012). [https://doi.org/10.1007/JHEP07\(2012\)161](https://doi.org/10.1007/JHEP07(2012)161).
- [47] M. Archidiacono, N. Fornengo, C. Giunti, and A. Melchiorri, *Testing 3+1 and 3+2 neutrino mass models with cosmology and short baseline experiments*, Phys. Rev. D86 (2012) 065028. <https://doi.org/10.1103/PhysRevD.86.065028>.
- [48] E. Akhmedov and T. Schwetz, *MiniBooNE and LSND data: non-standard neutrino interactions in a (3+1) scheme versus (3+2) oscillations*, J. High Energ. Phys. 2010, 115 (2010). [https://doi.org/10.1007/JHEP10\(2010\)115](https://doi.org/10.1007/JHEP10(2010)115).
- [49] J. Liao and D. Marfatia, *Impact of nonstandard interactions on sterile neutrino searches at IceCube*, Phys. Rev. Lett. 117 (2016) 071802. <https://doi.org/10.1103/PhysRevLett.117.071802>.

- [50] K. S. Babu, D. W. McKay, I. Mocioiu, and S. Pakvasa, *Light Sterile Neutrinos, Lepton Number Violating Interactions and the LSND Anomaly*, Phys. Rev. D93 (2016) 113019. <https://doi.org/10.1103/PhysRevD.93.113019>.
- [51] M. Blennow *et. al.*, *Non-Unitarity, sterile neutrinos, and Non-Standard neutrino Interactions*, J. High Energ. Phys. 2017, 153 (2017). [https://doi.org/10.1007/JHEP04\(2017\)153](https://doi.org/10.1007/JHEP04(2017)153)
- [52] A. Esmaili and H. Nunokawa, *On the robustness of IceCube's bound on sterile neutrinos in the presence of non-standard interactions*, Eur. Phys. J. C 79, 70 (2019). <https://doi.org/10.1140/epjc/s10052-019-6595-9>.
- [53] S. N. Gninenco, *Sterile neutrino decay as a common origin for LSND/MiniBooNe and T2K excess events*, Phys. Rev. D 85 (2012) 051702. <https://doi.org/10.1103/PhysRevD.85.051702>.
- [54] S. N. Gninenco, *New limits on radiative sterile neutrino decays from a search for single photons in neutrino interactions*, Phys. Lett. B 710 (2012) 86. <https://doi.org/10.1016/j.physletb.2012.02.071>.
- [55] R. Krishnan, A. Mukherjee and S. Goswami, *Realization of the minimal extended seesaw mechanism and the TM_2 type neutrino mixing*, J. High Energ. Phys. 2020, 50 (2020). [https://doi.org/10.1007/JHEP09\(2020\)050](https://doi.org/10.1007/JHEP09(2020)050).
- [56] J. Barry, W. Rodejohann and H. Zhang, *Light Sterile Neutrinos: Models and Phenomenology*, J. High Energ. Phys. 2011, 91 (2011). [https://doi.org/10.1007/JHEP07\(2011\)091](https://doi.org/10.1007/JHEP07(2011)091).
- [57] J. Barry, W. Rodejohann and H. Zhang, *Sterile Neutrinos for Warm Dark Matter and the Reactor Anomaly in Flavor Symmetry Models*, <https://doi.org/10.1088/1475-7516/2012/01/052>, JCAP 1201 (2012) 052.
- [58] H. Zhang, *Light Sterile Neutrino in the Minimal Extended Seesaw*, Phys. Lett. B 714 (2012) 262. <https://doi.org/10.1016/j.physletb.2012.06.074>.
- [59] D. Borah, *Non-zero θ_{13} with Unbroken $\mu - \tau$ Symmetry of the Active Neutrino Mass Matrix in the Presence of a Light Sterile Neutrino*, Phys. Rev. D 95 (2017) 035016. <https://doi.org/10.1103/PhysRevD.95.035016>.
- [60] P. Das, A. Mukherjee, M. K. Das, *Active and sterile neutrino phenomenology with A_4 based minimal extended seesaw*, Nucl. Phys. B 941 (2019) 755. <https://doi.org/10.1016/j.nuclphysb.2019.02.024>.
- [61] Neelakshi Sarma, Kalpana Bora, Debasish Borah, *Compatibility of A_4 Flavour Symmetric Minimal Extended Seesaw with (3+1) Neutrino Data*, Eur. Phys. J. C 79 2 (2019) 129. <https://doi.org/10.1140/epjc/s10052-019-6584-z>.
- [62] D. Suematsu, *A light sterile neutrino based on the seesaw mechanism*, Prog.Theor.Phys. 106 (2001) 587. <https://doi.org/10.1143/PTP.106.587>.
- [63] R. N. Mohapatra, *Connecting bimaximal neutrino mixing to a light sterile neutrino*, Phys.Rev. D 64 (2001) 091301. <https://doi.org/10.1103/PhysRevD.64.091301>.
- [64] K.S. Babu, G. Seidl, *Simple Model for (3+2) Neutrino Oscillations*, Phys.Lett. B 591 (2004) 127. <https://doi.org/10.1016/j.physletb.2004.03.086>.

- [65] R.N. Mohapatra, S. Nasri, Hai-Bo Yu, *Seesaw Right Handed Neutrino as the Sterile Neutrino for LSND*, Phys. Rev. D 72 (2005) 033007. <https://doi.org/10.1103/PhysRevD.72.033007>.
- [66] A. C. B. Machado, V. Pleitez, *Quasi-Dirac neutrinos in a model with local B-L symmetry*, J. Phys. G: Nucl. Part. Phys. 40 (2013) 035002. <https://doi.org/10.1088/0954-3899/40/3/035002>.
- [67] M. Ghosh, S. Goswami, S. Gupta, *Two-Zero mass matrices and sterile neutrinos*, J. High Energ. Phys. 2013, 103 (2013). [https://doi.org/10.1007/JHEP04\(2013\)103](https://doi.org/10.1007/JHEP04(2013)103).
- [68] Y. Zhang, *Majorana neutrino mass matrices with three texture zeros and the sterile neutrino*, Phys. Rev. D 87 (2013) 053020. <https://doi.org/10.1103/PhysRevD.87.053020>.
- [69] Y. Zhang, X. Ji and R. N. Mohapatra, *A Naturally Light Sterile neutrino in an Asymmetric Dark Matter Model*, J. High Energ. Phys. 2013, 104 (2013). [https://doi.org/10.1007/JHEP10\(2013\)104](https://doi.org/10.1007/JHEP10(2013)104).
- [70] M. Frank and L. Selbuz, *Sterile neutrinos in $U(1)'$ with R-parity Violation*, Phys. Rev. D 88 (2013) 055003. <https://doi.org/10.1103/PhysRevD.88.055003>.
- [71] D. Borah and R. Adhikari, *Common Radiative Origin of Active and Sterile Neutrino Masses*, Phys. Lett. B 729 (2014) 143. <https://doi.org/10.1016/j.physletb.2014.01.018>.
- [72] A. Merle, S. Morisi, W. Winter, *Common origin of reactor and sterile neutrino mixing*, J. High Energ. Phys. 1407 (2014) 039. [https://doi.org/10.1007/JHEP07\(2014\)039](https://doi.org/10.1007/JHEP07(2014)039).
- [73] Newton Nath, Monojit Ghosh, Shivani Gupta, *Understanding the Masses and Mixings of One-Zero Textures in 3+1 Scenario*, Int. J. Mod. Phys. A 31 (2016) 1650132. <https://doi.org/10.1142/S0217751X16501323>.
- [74] D. Borah *et. al.*, *Analysis of four-zero textures in 3+1 framework*, Phys. Rev. D 94 (2016) 113001. <https://doi.org/10.1103/PhysRevD.94.113001>.
- [75] D. Borah, *Light Sterile Neutrino and Dark Matter in Left-Right Symmetric Models Without Higgs Bidoublet*, Phys. Rev. D94 (2016) 075024. <https://doi.org/10.1103/PhysRevD.94.075024>.
- [76] S. Dev, D. Raj, R. R. Gautam, *Deviations in Tribimaximal Mixing From Sterile Neutrino Sector*, Nucl. Phys. B 911 (2016) 744. <https://doi.org/10.1016/j.nuclphysb.2016.08.015>.
- [77] N. Nath, M. Ghosh, S. Goswami and S. Gupta, *Phenomenological study of extended seesaw model for light sterile neutrino*, J. High Energ. Phys. 1703 (2017) 075. [https://doi.org/10.1007/JHEP03\(2017\)075](https://doi.org/10.1007/JHEP03(2017)075).
- [78] D. Borah, M. Ghosh, S. Gupta and S. K. Raut, *Texture zeros of low-energy Majorana neutrino mass matrix in 3+1 scheme*, Phys. Rev. D 96 (2017) 055017. <https://doi.org/10.1103/PhysRevD.96.055017>.
- [79] Imtiyaz Ahmad Bhat, Rathin Adhikari, *Dark matter mass from relic abundance, an extra $U(1)$ gauge boson, and active-sterile neutrino mixing*, Phys. Rev. D 101 (2020) 075030. <https://doi.org/10.1103/PhysRevD.101.075030>.
- [80] C. A. de S. Pires, *A cosmologically viable eV sterile neutrino model*. <https://doi.org/10.1016/j.physletb.2019.135135>.
- [81] Priyanka Kumar, Mahadev Patgiri, *Minimal extended seesaw and group symmetry realization of two-zero textures of neutrino mass matrices*, Nucl.Phys. B957 (2020) 115082.

- [https://doi.org/10.1016/j.nuclphysb.2020.115082.](https://doi.org/10.1016/j.nuclphysb.2020.115082)
- [82] João Paulo Pinheiro, C. A. de S. Pires, *Vacuum stability and spontaneous violation of the lepton number at low energy scale in a model for light sterile neutrinos*, Phys. Rev. D 102 (2020) 015015.<https://doi.org/10.1103/PhysRevD.102.015015>.
- [83] V. V. Vien, *3+1 active–sterile neutrino mixing in B-L model with $S_3 \times Z_4 \times Z_2$ symmetry for normal neutrino mass ordering*, Eur. Phys. J. C 81 (2021) 416. <https://doi.org/10.1140/epjc/s10052-021-09214-5>.
- [84] R. E. Marshak and R. N. Mohapatra, *Quark - Lepton Symmetry and B-L as the U(1) Generator of the Electroweak Symmetry Group*, Phys. Lett. 91B (1980) 222. [https://doi.org/10.1016/0370-2693\(80\)90436-0](https://doi.org/10.1016/0370-2693(80)90436-0).
- [85] C. Wetterich, *Neutrino masses and the scale of B-L violation*, Nucl. Phys. B 187 (1981) 343. [https://doi.org/10.1016/0550-3213\(81\)90279-0](https://doi.org/10.1016/0550-3213(81)90279-0).
- [86] W. Abdallah, D. Delepine, S. Khalil, *TeV Scale Leptogenesis in B-L Model with Alternative Cosmologies*, Phys.Lett. B 725 (2013) 361. <https://doi.org/10.1016/j.physletb.2013.07.047>.
- [87] C. Pallis, Q. Shafi, *Update on Minimal Supersymmetric Hybrid Inflation in Light of PLANCK*, Physics Letters B 725 (2013) 327. <https://doi.org/10.1016/j.physletb.2013.07.029>.
- [88] W. Buchmüllera, V. Domcke, K. Kamadac, K. Schmitzd, *Hybrid Inflation in the Complex Plane*, JCAP07 (2014) 054. <https://doi.org/10.1088/1475-7516/2014/07/054>.
- [89] A. Moursy, *No-scale gauge non-singlet inflation inducing TeV scale inverse seesaw mechanism*, J. High Energ. Phys. 2021, 208 (2021). [https://doi.org/10.1007/JHEP10\(2021\)208](https://doi.org/10.1007/JHEP10(2021)208).
- [90] K. Aoki, T. Q. Loc, T. Noumi, and J. Tokuda, *Is the Standard Model in the Swampland? Consistency Requirements from Gravitational Scattering*, Phys. Rev. Lett. 127 (2021) 091602, <https://doi.org/10.1103/PhysRevLett.127.091602>.
- [91] A. Davidson, *B – L as the fourth color within an $SU(2)_L \times U(1)_R \times U(1)$ model*, Phys. Rev. D 20 (1979) 776. <https://doi.org/10.1103/PhysRevD.20.776>.
- [92] R. N. Mohapatra and R. E. Marshak, *Local B – L Symmetry of Electroweak Interactions, Majorana Neutrinos, and Neutron Oscillations*, Phys. Rev. Lett. 44 (1980) 1316. <https://doi.org/10.1103/PhysRevLett.44.1316>.
- [93] S. Khalil, *Low scale B-L extension of the Standard Model at the LHC*, J. Phys. G 35 (2008) 055001. <https://doi.org/10.1088/0954-3899/35/5/055001>.
- [94] M . Abbas, S. Khalil, *Neutrino masses, mixing and leptogenesis in TeV scale B-L extension of the standard model*, J. High Energ. Phys.04 (2008) 056. <https://doi.org/10.1088/1126-6708/2008/04/056>.
- [95] S. Iso, N. Okada and Y. Oriksasa, *Classically Conformal B-L extended Standard Model*, Phys. Lett. B 676 (2009) 81. <https://doi.org/10.1016/j.physletb.2009.04.046>.
- [96] S. Iso, N. Okada and Y. Oriksasa, *The minimal B-L model naturally realized at TeV scale*, Phys. Rev. D 80 (2009) 115007. <https://doi.org/10.1103/PhysRevD.80.115007>.

- [97] N. Sahu and U. A. Yajnik, *Dark matter and leptogenesis in gauged B-L symmetric models embedding ν MSM*, Phys. Lett. B635 (2006) 1116. <https://doi.org/10.1016/j.physletb.2006.02.040>.
- [98] W. Emam, S. Khalil, *Higgs and Z! Phenomenology in B-L extension of the Standard Model at LHC*, Eur.Phys.J.C 55 (2007) 625. <https://doi.org/10.1140/epjc/s10052-007-0411-7>.
- [99] T. Basak and T. Mondal, *Constraining Minimal $U(1)_{B-L}$ model from Dark Matter Observations*, Phys. Rev. D 89 (2014) 063527. <https://doi.org/10.1103/PhysRevD.89.063527>.
- [100] W. Rodejohann and C. E. Yaguna, *Scalar dark matter in the B-L model*, JCAP 1512 (2015) 032. <https://doi.org/10.1088/1475-7516/2015/12/032>.
- [101] J. Guo, Z. Kang, P. Ko, and Y. Orikasa, *Accidental Dark Matter: Case in the Scale Invariant Local B-L Models*, Phys. Rev. D 91 (2015) 115017. <https://doi.org/10.1103/PhysRevD.91.115017>.
- [102] A. El-Zant, S. Khalil, and A. Sil, *Warm Dark Matter in B-L Inverse Seesaw*, Phys. Rev. D 91 (2015) 035030. <https://doi.org/10.1103/PhysRevD.91.035030>.
- [103] S. Khalil, H. Okada, *Dark Matter in B-L Extended MSSM Models*, Phys.Rev.D 79 (2009) 083510. <https://doi.org/10.1103/PhysRevD.79.083510>.
- [104] T. Higaki, R. Kitano, R. Sato, *Neutrinoful Universe*, J. High Energ. Phys. 2014, 44 (2014). [https://doi.org/10.1007/JHEP07\(2014\)044](https://doi.org/10.1007/JHEP07(2014)044).
- [105] P. S. B. Dev, R. N. Mohapatra, Y. Zhang, *Leptogenesis constraints on B- L breaking Higgs boson in TeV scale seesaw models*, J. High Energ. Phys. 2018, 122 (2018). [https://doi.org/10.1007/JHEP03\(2018\)122](https://doi.org/10.1007/JHEP03(2018)122).
- [106] T. Hasegawa, N. Okada and O. Seto, *Gravitational waves from the minimal gauged $U(1)_{B-L}$ model*, Phys. Rev. D 99 (2019) 095039. <https://doi.org/10.1103/PhysRevD.99.095039>.
- [107] H. Ishimori *et. al.*, *Non-Abelian Discrete Symmetries in Particle Physics*, Prog. Theor. Phys. Suppl. 183 (2010) 1. <https://doi.org/10.1143/PTPS.183.1>.
- [108] P. A. Zyla *et al.* (Particle Data Group), *Review of Particle Physics*, Prog. Theor. Exp. Phys. 2020, 083C01 (2020). <https://doi.org/10.1093/ptep/ptaa104>.
- [109] C. Jarlskog, *Commutator of the Quark Mass Matrices in the Standard Electroweak Model and a Measure of Maximal CP Nonconservation*, Phys. Rev. Lett. 55 (1985) 1039. <https://doi.org/10.1103/PhysRevLett.55.1039>.
- [110] D.-d. Wu, *Rephasing invariants and CP violation*, Phys. Rev. D 33 (1986) 860. <https://doi.org/10.1103/PhysRevD.33.860>.
- [111] O.W. Greenberg, *Rephasing invariant formulation of CP violation in the Kobayashi-Maskawa framework*, Phys. Rev. D32 (1985) 1841. <https://doi.org/10.1103/PhysRevD.32.1841>.
- [112] M. Mitra, G. Senjanovic, F. Vissani, *Neutrinoless Double Beta Decay and Heavy Sterile Neutrinos*, Nucl. Phys. B 856 (2012) 26. <https://doi.org/10.1016/j.nuclphysb.2011.10.035>.
- [113] W. Rodejohann, *Neutrinoless double beta decay and neutrino physics*, J. Phys. G39 (2012) 124008. <https://doi.org/10.1088/0954-3899/39/12/124008>.

- [114] J. D. Vergados, H. Ejiri and F. Simkovic, *Theory of neutrinoless double beta decay*, Rep. Prog. Phys. 75 (2012) 106301. <https://doi.org/10.1088/0034-4885/75/10/106301>.
- [115] F. Capozzi *et. al.*, *Global constraints on absolute neutrino masses and their ordering*, Phys. Rev. D 95 (2017) 096014. <https://doi.org/10.1103/PhysRevD.95.096014>.
- [116] P. de Salas *et. al.*, *Status of neutrino oscillations 2018: 3σ hint for normal mass ordering and improved CP*, Phys. Lett. B 782 (2018) 633. <https://doi.org/10.1016/j.physletb.2018.06.019>.
- [117] I. Esteban, M.C. Gonzalez-Garcia and M. Maltoni, *Global analysis of three-flavour neutrino oscillations: synergies and tensions in the determination of θ_{23} , δ_{CP} , and the mass ordering*, J. High Energ. Phys. 2019 (2019) 55. [https://doi.org/10.1007/JHEP01\(2019\)106](https://doi.org/10.1007/JHEP01(2019)106).
- [118] Kevin J. Kelly *et. al.*, *Neutrino mass ordering in light of recent data*, Phys. Rev. D 103 (2021) 013004. <https://doi.org/10.1103/PhysRevD.103.013004>.
- [119] M. Agostini *et al.* (GERDA Collaboration), *Improved limit on neutrinoless double beta decay of ^{76}Ge from GERDA Phase II*, Phys. Rev. Lett. 120 (2018) 132503. <https://doi.org/10.1103/PhysRevLett.120.132503>.
- [120] C. E. Aalseth *et al.* (Majorana Collaboration), *Search for Zero-Neutrino Double Beta Decay in ^{76}Ge with the Majorana Demonstrator*, Phys. Rev. Lett. 120 (2018) 132502. <https://doi.org/10.1103/PhysRevLett.120.132502>.
- [121] C. Alduino *et al.* (CUORE collaboration), *First Results from CUORE: A Search for Lepton Number Violation via $0\nu\beta\beta$ Decay of ^{130}Te* , Phys. Rev. Lett. 120 (2018) 132501. <https://doi.org/10.1103/PhysRevLett.120.132501>.
- [122] A. Gando *et al.* (KamLAND-Zen Collaboration), Phys. Rev. Lett. 117 (2016) 082503.
- [123] M. Agostini *et al.* (GERDA Collaboration), *Probing Majorana neutrinos with double- β decay*, Science 365 (2019) 1445. DOI:10.1126/science.aav8613.
- [124] D. Adams *et al.* (CUORE collaboration), *Improved Limit on Neutrinoless Double-Beta Decay in ^{130}Te with CUORE*, Phys. Rev. Lett. 124 (2020) 122501. <https://doi.org/10.1103/PhysRevLett.124.122501>.
- [125] E. Armengaud *et al.* (CUPID-Mo Collaboration), *New Limit for Neutrinoless Double-Beta Decay of ^{100}Mo from the CUPID-Mo Experiment*, Phys. Rev. Lett. 126 (2021) 181802. <https://doi.org/10.1103/PhysRevLett.126.181802>.